CHALMERS

Development of a low-cost laser range-finder (LIDAR)

Master's Thesis in Systems, Control and Mechatronics

Peter Kaldén

Erik Sternå

Department of Microtechnology & Nanoscience
Chalmers University of Technology
Gothenburg, Sweden 2015
Master's Thesis 2015

Abstract

This is a development report that covers the work attempting to design and construct a laser based LIDAR. The goal of the project was to design a cheap laser range-finder capable of performing scanning measurements. This was intended to be an open-source sensor primarily aimed at engineers lacking a cost-viable sensor for positioning. The target specifications of the system were to have a measurement range from 0.5 m to 5 m with a measurement accuracy of 0.05 m. Scanning was initially specified but was removed form the scope due to time constraints. The requirements to be able to handle scanning measurements were however retained to enable scanning to be realized at a later time. Scanning with a 360 degrees field of view with a 1 degree angular resolution was specified, making a measurement rate of at least 3.6 kHz a requirement. The total cost limit set was €120.

The major part of this thesis discusses the selection of suitable components and the reasoning behind their choice. During the component selection process, the focus was primarily to minimize component costs and to adhere to international safety-regulations while still fulfilling the specifications. Since the goal was to make this project open source the reasoning and process of development is vital for anyone wishing to continue the development. The selected components were assembled and tested. The approximated total cost of the components for the system ended at €125, slightly higher than the cost limit without any manufacturing cost included. It is however close to the limit and it might be possible to reduce the cost with alternative components. The control system, the time measurement, the transmitter and the optics were all verified working and fulfilling their part of the specifications. However the detector and amplifier were unable to receive and amplify the very weak return signal preventing the system from being verified in its entirety.

Contents

Abbreviations

Glossary

laser Light amplification by stimulation of radiation. 5, 13, 14

LIDAR Light detection and ranging. 1, 5, 6, 22, 34–36, 46, 50, 51

microcontroller Small processor with embedded memory and peripheral I/O systems. 7, 10, 12, 33, 34, 36, 38, 45, 48–51, 55, 61

Acronyms

ADC Analog-to-Digital Converter. 9, 34, 38

APD Avalanche Photo-diode. 26, 33, 51

ASIC Application-specific integrated circuit. 7, 33

CTMU Charge Time Measurement Unit. 7, 33

DAC Digital-to-Analog Converter. 34, 38

GaAs Gallium Arsenide. 13, 14

IEC International Electrotechnical Commission. 14

LED Light Emitting Diode. 6

MEMS Microelectromechanical systems. 9

MOSFET Metal-oxide-semiconductor field-effect transistor. 16, 17, 45, 64

MPE Maximum permissible exposure. 14, 15

NEP Noise-equivalent power. 26, 27

OP-amp Operational Amplifier. 29–32, 37, 38, 46, 48, 59, 63

PCB Printed Circuit Board. 28, 34, 36–38, 40, 46, 48, 51, 55–58

PWM Pulse width modulation. 16

RMS Root mean square. 31

SNR Signal-to-noise ratio. 26, 27, 29–33

SPI Serial Peripheral Interface. 34

TDC Time-to-Digital Converter. 7, 12, 33, 34, 36, 38, 48–50

TMU Time Measurement Unit. 7, 33

ToF Time of flight. 2, 7, 11, 12

ToS Time of sight. 9

UART Universal Asynchronous Receiving and Transmitting. 6, 34

VCSEL Vertical-cavity surface-emitting laser. 13

Introduction

In the world of robotics and autonomous vehicles, the ability to sense the environment is very important. Technologies based on cameras, such as the Microsoft Kinect[1], can be used to gather lots of information about the environment. However, this information may be hard to process due to the fact that it requires a large amount of computing power to analyse. Also, dependent on the technology used, the range might be very limited or the frame-rate low.

Instead, LIDARs can be used. A LIDAR uses light to measure the distance to an object. Certain LIDARs can also measure distance at several angles by rotating parts of the measurement device for example, thus achieving a plane of sensor information. The measurement area can therefore be wide angled (up to 360° field of view is available). On the market, LIDARs are available from several companies such as SICK and Hokuyo[2, 3], but at a price which most hobbyists and schools cannot afford. Also, they are often closed source and generally do not offer the customer much possibility for tweaking parameters such as sample rate, angular resolution, output power and so on. The high cost of LIDARs today limits the potential for technological development in the field of robotics and autonomous vehicles. This is what this master thesis project hopes to change. What this project aims to do is to build a functional, low-cost and easy-to-use LIDAR using a laser with a performance usable for a wide range of applications. Initially the goal also specified that the LIDAR should be scanning, i.e. rotating to do measurements in a plane. This goal was deemed too time consuming and was removed, however the specifications remain so that scanning might be realized without major changes. The goal of the project is to develop a system that fulfils the goals stated in table 1.

Parameter	Abbreviation	Value
Max detection range	L_{max}	5 m
Min detection range	L_{min}	0.5 m
Measurement accuracy [1]	L_{res}	±0.05 m
Angular detection span	φ_A	360°
Angular resolution	φ_r	1°
Scanning frequency	f_{scan}	10 Hz
Measurement Frequency	f_{meas}	3600 Hz

Table 1: *Target performance parameters of the system*

- The LIDAR should also fulfil the following criteria:
  1 Not cost more than 1000 SEK (approx €120) to manufacture.
  2 Easy to use for hobbyists (support of standard interfaces such as Universal Asynchronous Receiving and Transmitting (UART) and USB).
  3 Open-source hardware and software, thus allowing other hobbyists and researchers to further develop the sensor.
  4 Well-written and extensive documentation, to allow for easy integration and further development.
  5 Give the user high control and customizability when communicating with the sensor, such as setting the updating frequency, angular resolution, measuring area and so on, thus letting the user optimize the sample rate/resolution dilemma to fit their application.
  6 Contain some higher level functions, such as object detection.
  7 Safe according to international laser safety regulations.
- A long-term goal is that the LIDAR developed should be commercially available for people all over the world

1 Review and Overview

1.1 Review of distance measurement techniques

The main reason for using a laser is that a laser-beam does not diverge significantly making it possible to use a narrow beam to make a point measurement regardless of the distance to the object detected. A laser also has the advantage of having a very narrow bandwidth with regards to its wavelength, making it possible to have a narrow bandwidth receiver making it less sensitive to ambient noise. Lasers are also generally able to operate on a higher frequency than Light Emitting Diodes (LEDs), which makes them more well suited for high-speed measurements. Some different approaches to measure distance using a laser were investigated and evaluated after which one method was chosen.

1.1.1 Time-of-Flight

This method is one of the most used and straight-forward solutions. The concept is simple: A pulse of light is sent out and the time until the reflected pulse is detected is measured. By using pulses the power of the emitted signal can be greater than if it was continuous, making the return signal stronger. A conceptual image can be found in figure 1.

[1]When calculating the requirements on the measurement methods evaluated, this figure is used as resolution requirement, since a resolution of at least 0.05 m is needed to get an accuracy of 0.05 m

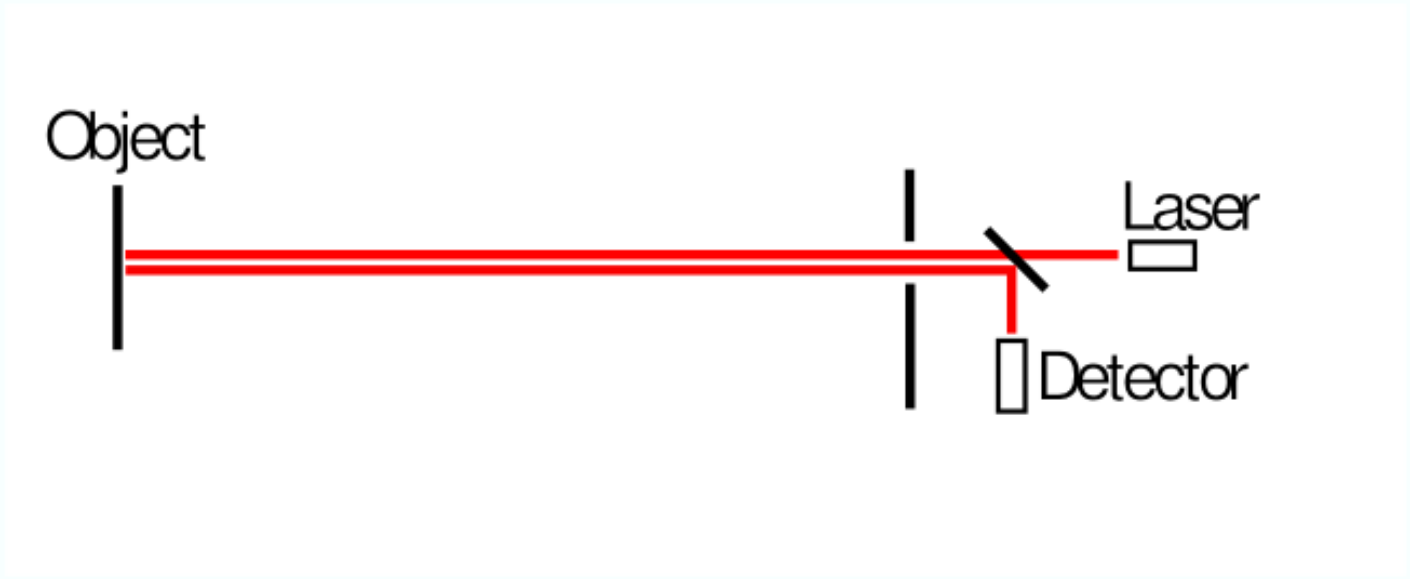

Figure 1: *Conceptual image of ToF*

Since light travels very fast, the requirement on resolution of the sampling is very high. The minimum required time sampling resolution can be calculated as seen in equation 1

$$T_{R,ToF} = \frac{2 * L_{res}}{c} \approx \frac{2 * 0.05\,m}{3 * 10^8\,m/s} \approx 333\,ps \tag{1}$$

where c is the speed of light, L_{res} is the required distance resolution (as defined as one of the target parameters in table 1) and $T_{R,ToF}$ is the required time resolution. The factor 2 in the formula represents the fact that light has to travel to the target and back.
There are several ways to measure time precisely. Many companies manufacturing laser range finders that use this technology design their own Application-specific integrated circuits (ASICs) which is way over the budget and out of scope for this project. There are however some integrated circuits capable of this, so called Time-to-Digital Converters (TDCs) or Time Measurement Units (TMUs) but they are generally rare and expensive [4, 5]. Another solution could be to design a circuit for this using a capacitor and a constant current source. The charge in the capacitor will then correspond to a time. Some microcontrollers (such as Microchips PIC microcontrollers) have such a module (called Charge Time Measurement Unit (CTMU)) built-in, which is rather easy to use [6]. However an inquiry at a TDC-manufacturing company revealed that there were TDC-circuits with a time resolution of 45 ps available at approximately €10.

1.1.2 Triangulation

This is a common method when it comes to range-finding, both with lasers and light in general[7]. It is conceptually simple but may require more advanced optics than the other solutions. The laser light is sent out and is reflected back to a sensor array that is positioned in the same plane, at a distance from the emitter (distance a in figure 2). The point on the sensor array where the signal is received determines the distance to the object. The relation between the distance, sensor position

and the signal position on the sensor array can be found in equation 2:

$$L = \frac{a * f}{x} \tag{2}$$

where L is the distance to the object, a is the distance between the focal point of the lens and the laser output, f is the focal length and x is the position on the sensor array. A conceptual image is shown in figure 2.

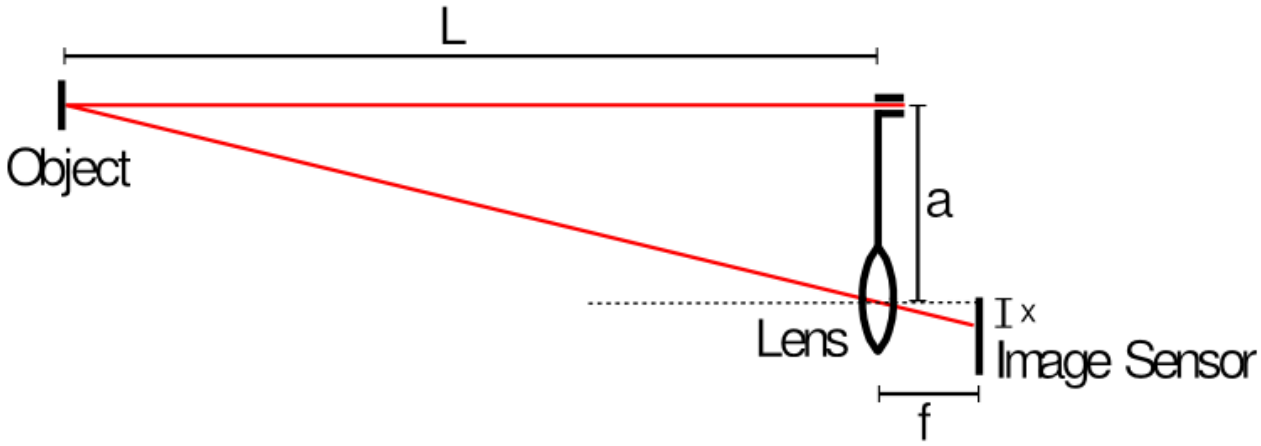

Figure 2: *Conceptual image of triangulation*

The measurement time is decided by the integration time of the sensor, i.e. the time it takes to determine the value of each sensor in the array. An example sensor was found [8] that has an integration time over the whole array of 33.75 μs. Comparing this time to the time available for each measurement: $1/f_{meas} = 277.8\ \mu s > 33.75\ \mu s$, ($f_{meas}$ being the measurement frequency defined in the target specification found in table 1), we found that this is more than enough time and would allow for several measurements on each point to increase the accuracy. Using this sensor would be entirely feasible from a measurement time point of view. The laser beam needs to be continuous for the time it takes for the sensor time to take in the return signal, limiting the output power, in turn limiting the return signal.

The resolution depends on the number of sensors on the array, the sensor spacing of the array, the distance between the sensor and the laser emission point (shown as a in figure 2) as well as the optics solution. The distance calculation formula can be rewritten to calculate the required resolution of the sensor array. This can be done by calculating the difference in position of the returned light at the sensor for two values at the maximum measurement distance, as shown in equation 3.

$$\Delta x_{L_{max}} = \frac{a * f}{L_{max}} - \frac{a * f}{L_{max} - L_{res}} \tag{3}$$

where a is the distance between emitter and the focusing lens and assumed to be 0.05 m, f is the distance from the lens to the sensor and assumed to be 0.05 m. L_{max} and L_{res} is the max measurement distance and the required resolution respectively as can be seen in table 1. This requirement presents a problem: 5 μm is close to the wavelength of the laser and it is therefore possible that the properties of the laser beam will prevent this resolution being possible at all. The example sensor array has 63.5 μm center to center spacing. This means that it is has a

lower resolution than needed. However the sensor array reports the analog values of each sensor and therefore interpolation can be used to increase this resolution. The theoretical maximum interpolation is determined by the resolution of the Analog-to-Digital Converter (ADC) used to sample, the power distribution of the laser beam and the assumption that the laser spot is equal to or larger than the size of a pixel. Given an ADC with 12-bits each pixel can have 4096 different values. This means that the center of the laser point can in theory be determined at a 4096-part of a pixel, which is equal to 0.015 μm in this case and therefore enough in theory. A more realistic assumption is that the value can be interpolated by a factor 10-100 instead of 4096, meaning that the example sensor would not work in that aspect. However, given another sensor array with tighter pixels or a shorter maximum distance it could be made to work.

The biggest unique cost for this solution would be the sensor, since one such sensor costs about €15 [8]. There are several types of such sensor arrays, but this is a cheap example which might be to fulfil the requirements.

1.1.3 Time-of-Sight

Time of sight (ToS) is a method that works by sweeping a laser beam over the measurement span away from the sensor. By sweeping with a constant angular velocity and measuring the timing of where in the sweep the laser is reflected into a narrow sensor slot the distance to the object can be calculated. It was inspired by a hobby project[9] and presents an interesting approach. A conceptual image is shown in figure 3

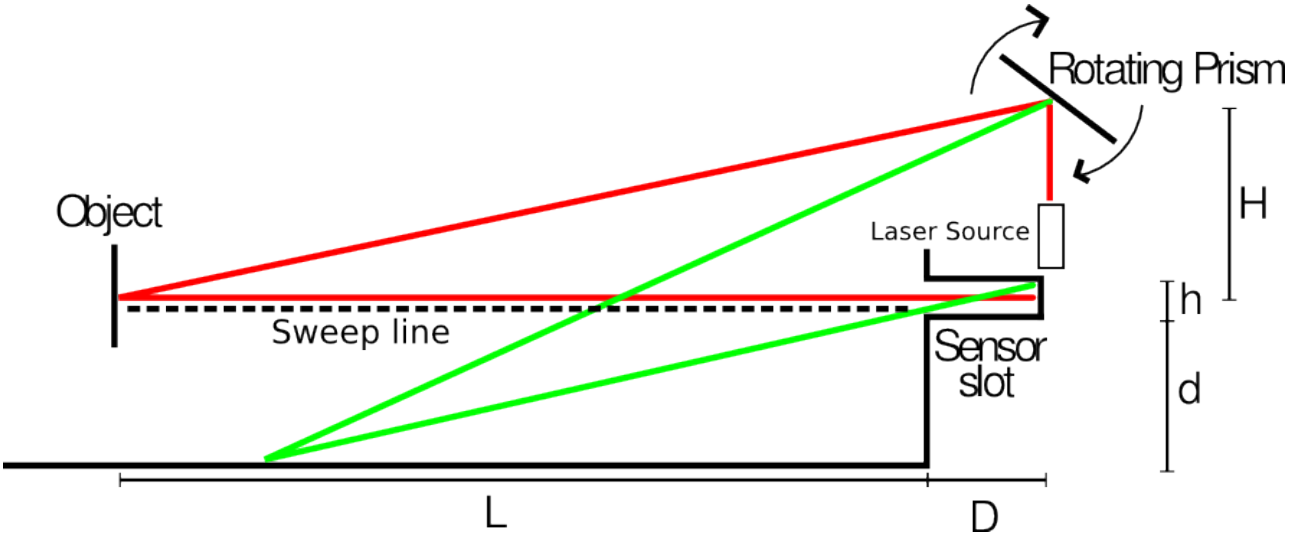

Figure 3: *Conceptual image of ToS*

The method requires that the laser beam is swept across the entire measurement span to perform a measurement. Sweeping the laser beam can be accomplished in multiple ways, the simplest being to use a rotating mirror or prism. The laser is reflected off the prism and the rotation is used to angle the reflection so that it sweeps. This can also be done via a so called Microelectromechanical systems (MEMS) mirror which is a small electrically controlled mirror. However they are expensive, rare and have a limited angular range which limits the sweep angle.

If a prism is used to sweep the laser, the prism must complete a rotation for each measurement. If

the prism is multi-sided, multiple smaller sweeps can be performed per rotation, reducing the requirement on the rotational speed of the prism. The required rotational speed f_{rot} can be calculated using equation 4.

$$f_{rot} = f_{meas}/n \tag{4}$$

where f_{meas} is the measurement rate defined in the target specification and n is the number of sides of the prism used. For a prism with $n = 1$ sides the rotational speed requirement becomes 3600 Hz or 216 000 rpm, which is unreasonably fast. For a 6-sided prism this becomes 600 Hz or 36 000 rpm, which is still faster than most motors run comfortably at. Most likely a sophisticated prism with many sides would be required for this method to work at the required sampling rate. This rotational speed can be converted into an angular velocity as shown in equation 5

$$\omega = (360 * f_{meas})/n \tag{5}$$

The angular velocity (ω) of the beam together with the angle difference at the maximum measurement distance sets the minimum sampling time. This because the desired resolution must be obtained at the maximum measurement distance. The angular difference at the maximum measurement distance is obtained as shown in equation 6, where H is the height from the sensor slot to the reflection point of the prism, shown in figure 3 and L_{max} and L_{res} are target specification parameters from table 1.

$$\Delta\varphi_{L_{max}} = \arctan(\frac{H}{L_{max} - L_{res}}) - \arctan(\frac{H}{L_{max}}) \tag{6}$$

The required sampling time can then be obtained using equation 7

$$T_s = \frac{\Delta\varphi_{L_{max}}}{\omega} \tag{7}$$

With a $H = 5\ cm$, $n = 6$ and L_{max}, L_{res} and f_{meas} as defined in table 1 the minimum sampling time becomes 26 ns. This is in the time realm where a microcontroller could reasonably be used to sample the time directly, which would reduce costs since a microcontroller would be used in any case for the interface and various calculations. The sensor slot dimensions also has some requirements. There is an issue where a ground reflection may produce a false reading if the sensor slot have insufficient height/length ratio, as can be seen by the green ray in figure 3. To eliminate this issue the condition in equation 8 needs to be satisfied.

$$\frac{d}{L_{max}} \leq \frac{h}{D} \tag{8}$$

If $d = 0.05\ m$ and $D = 0.05\ m$, then the aperture, h must satisfy the condition in equation 9

$$\begin{aligned} h &\leq \frac{D * d}{L_{max}} \\ h &\leq 0.0005\ m \end{aligned} \tag{9}$$

This aperture is to small to be reasonable because the total amount of photons would be too low to be able to trigger any reasonably priced sensor. A larger aperture can be compensated for by tilting the slot slightly upward from the ground. This worsens the resolution, and the height of the objects possible to detect at long ranges, but solves the problem of ground reflections and the larger aperture will let through more photons. This method would also require a very near continuous laser beam, making the possible output power of the laser low due to safety reasons.

1.1.4 Phase shift

This method was only briefly investigated at the end of the project to look for alternative solutions to include in the report. Therefore, phase shift was not considered at the choice of method.

Phase shift measurement uses a continuous laser beam that has an added sinusoidal power modulation. By calculating the phase difference between the laser pulse sent out and the one received from a reflecting target it is possible to partly calculate the distance to the target. Because the phase difference is periodic with the frequency of the power modulation, the distance can be deduced by multiple measurements using different modulation frequencies. Since several sequential measurements are required for each sample it might be difficult to achieve a high sampling rate.

The upside of this method is that the modulation is easy to measure since it is a continuous and predictable signal, it is also quite noise resistant and does not require a very fast photo-diode. Furthermore, very high resolution can be obtained, since if the modulation can be done at a high resolution. As with several of the other methods, there is the issue of using a continuous signal with respect to safety.

1.2 Choice of method

The method chosen was time of flight. The main argument against time of flight was initially the price of the specialized sampling circuits, but given that a time measurement module costs as little as €10 it might even be the cheapest solution. The sample frequency may be much higher than the other two methods which allows for a more accurate measurement result, by performing several measurements at each point. Using a pulsed laser allows for a higher output power, which gives a stronger return signal, while still keeping the system eye-safe. The optics are also easier than the other two solutions. What is harder is that the laser source must work at both high power and high frequency. The detection circuit also has to work at higher frequency, which requires more from the amplifiers and also on the PCB design itself.

1.3 Overview of ToF

As stated previously in section 1.1.1 the concept of time of flight is rather simple: send out a pulse of laser light and measure the time until the light pulse returns. The concept might be easy, but the details are tricky. The conceptual system design overview is shown in figure 4.

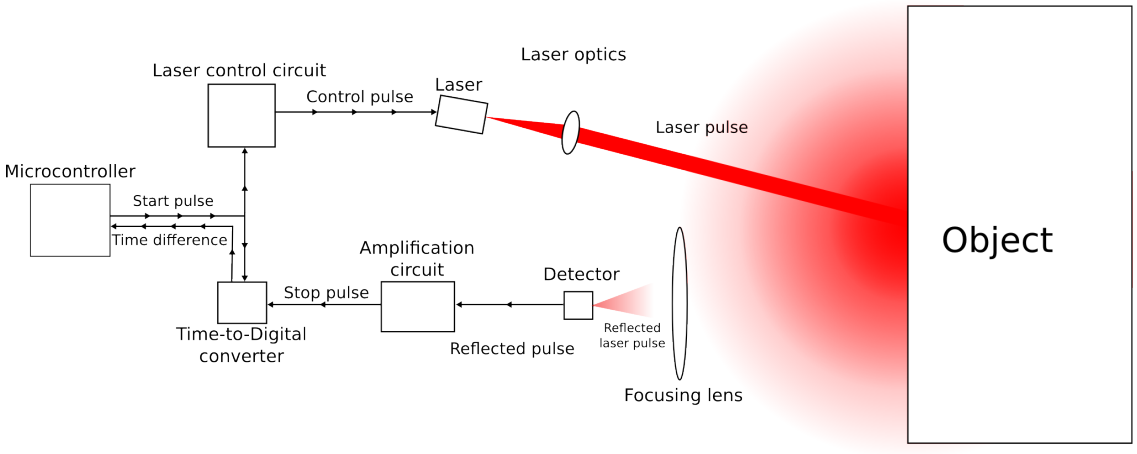

Figure 4: *Overview of the ToF system*

A microcontroller decides when to start measuring. It sends two carefully timed pulses: a control pulse to the laser driver and a start pulse to the TDC. The laser driver controls a laser source, which starts emitting light. The light may not be a perfect beam, depending on the laser type, so some laser optics are probably needed to shape the laser light into a nice beam and send it to an object. The target object reflects the light diffusively. The reflected light hits a lens which focuses the light into a detector. This signal is very weak, so a signal amplifying and conditioning circuit is needed. This circuit converts the weak signal from the photo-detector into a logic signal sent into the TDC, which stops the time measurement. The microcontroller reads the data from the TDC and performs some post-processing (such as filtering). This completes a full measurement cycle.

2 Development procedures

During the development, the main considerations when it came to choosing components were availability and price. The components had to be available to more or less anyone and the total budget must not be exceeded. This limited the choice of components, but also simplified the design procedure. Instead of calculating a theoretically ideal component, a search on major electronics distributors (such as Mouser, Farnell, Digi-key and RS-components) was made and some candidate component was selected. The components were then tested theoretically against the criteria on the component (based on information from the manufacturer) to check which would perform the best. These sources were also used to check the availability of components: If it couldn't be found at any of these suppliers, it probably didn't exist in the allowed price range. Also, more specialized suppliers and manufacturers (such as Edmund Optics, Thor Labs and Laser Components) were inquired to check the availability and price of some components. Since these companies are more specialized, components are often much more expensive, but a larger selection of special components is available.

2.1 Transmitter design

2.1.1 Laser type

To keep prices low, a common type of laser should be used. It is also important that the laser can supply high power in short pulses, since this gives the receiver a stronger return signal to work with. There are many types of laser sources available that can fulfil the requirements for this application. There are however only two types of laser sources which can reasonably be used, based mostly on how common they are and their usual size: solid state lasers and diode lasers (also called semiconductor lasers).

Solid state lasers use a crystal as a lasing medium and two reflecting mirrors. They are powered optically from a diode laser or a flash-lamp. This structure makes them hard to control since it requires an understanding of the specific laser crystal's characteristics, but if properly controlled could most likely work. However they are likely to be very expensive unless one could find a pre-assembled module, especially if a specific wavelength is required (for example if a good sensor sensitive to a specific wavelength is found).

Diode lasers use a Gallium Arsenide (GaAs) structure as a gain medium and is powered directly with electrical current making them easy to control and supply power to. They are quite cheap, which is a major motivation to choose them as well as the small size, which is also preferable in this application. They do however deliver a beam quality that is inferior to the solid state lasers and require a lens to function as a laser beam.

It was was decided that a laser diode would be used based on their price and ease of use. However there are several subtypes of laser diodes, the most significant ones being edge emitting laser diodes and Vertical-cavity surface-emitting laser (VCSEL) diodes.

Edge emitting laser diodes are cheap and easy to manufacture but they produce an elliptical beam rather than a round beam. They are also easily scalable in terms of output power by simply stacking parallel diodes in the same package.

VCSEL diodes are surface emitting diodes that use a quantum well design to produce a round laser beam. They can be tested before mounting, making them theoretically cheap. However, at the time of writing they are still being researched and are therefore not very widely available making them expensive.

Edge emitting laser diodes were chosen since minimizing cost was one of the main foci of this project. Using this kind of laser diode also gives a larger freedom while choosing the laser parameters, due to the commonness of this laser type.

2.1.2 Laser wavelength

The wavelength of the laser is an important property. Mainly, three different wavelength regions was considered: around 650 nm (visible red), 850-950 nm (near IR), 1550 nm (IR). All these wavelengths are rather standard wavelengths with different properties.

650 nm Light of this wavelength is visible without using any extra equipment. There will be dot (or line for a rotating system) on the target visible to the naked eye, which gives a great advantage during development, but the end user might not view this as an advantage. One problem is that narrow-band detectors are not very common for this wavelength. Furthermore, the laser diodes usually don't come in pulsed power specification, but rather only with constant power (and this means low power perhaps up to 100 mW).

850-950 nm The advantage of this region is that it is very commonly used, which means that there are lots of lasers and detectors to choose from in this region. Pulsed lasers are very common in this region, since many communication systems operate here. The fact that this wavelength region is common may also be a disadvantage since it means that many other applications also use these wavelengths which means that there probably is lots of noise in this part of the spectrum. Another disadvantage is that this wavelength region is especially dangerous for the eyes. These wavelengths are focused by the human eye and are invisible to the eye, which means that a person or animal hit by this, will not blink away. One good thing with this region is that detectors for this region can be made from silicon, which are generally cheaper than for example GaAs-based photo-detectors[10, 11].

1550 nm This is also a rather common wavelength in communication. The biggest advantage with this wavelength is that it is not focused by the human eye, making it very eye safe. Due to this, almost any amount of output power can be emitted, as long as the laser diode can handle it. Since this wavelength region is not as common as the other two regions, the cost is much greater. One reason for this might be that this wavelength cannot be easily achieved using laser diodes made using standard semiconductor techniques. Another downside is that detectors at this wavelength are rather uncommon and expensive, since they cannot be made from silicon[10].

The most reasonable wavelength to use is around 850-950 nm. The commonness of both lasers and detectors allows for a choice of better performance at the same price and allows for a wide variety of choices, despite the fact that it's the most "crowded" window and the possible eye hazard. Due to the eye-hazard, the output power has to be limited more compared to the other two considered regions.

Taking all these parameters into account a laser diode can now be selected. The one that was chosen was SPL PL90_0 from OSRAM, as it has the correct wavelength, a high output power, is designed for pulsed operation and is available at a rather low price.[12]

2.1.3 Laser safety

Since lasers can be harmful to the human body, particularly the eyes, it is necessary to calculate which laser pulses are harmful and which are not. A stronger laser pulse will give a stronger reflected pulse which is desirable since at longer distances this returned pulse will be very weak. The maximum safe laser power should be calculated to allow a pulse as powerful as possible while still having it remain eye-safe. Allowed laser radiation is determined by the guidelines set by the IEC 60825 standard developed by International Electrotechnical Commission (IEC)[13]. The allowed output power is always calculated in a worst-case scenario, which means that for this application, it is assumed that a user is standing and looking straight into the laser for an extended period of time, without turning away or blinking. Even if the system rotates, the worst case is still the same since the rotation might somehow stop. When calculating the Maximum permissible exposure (MPE) for laser light, three cases are considered: single pulse, average energy and pulse train. The key factors

here are the wavelength (λ), the pulse length (t_p), the pulse repetition frequency ($f_{rep} = \frac{1}{T_{rep}}$) and the total exposure time (T_{exp}). The wavelength is set to 900 nm, the total exposure time is set to a long time (about 30 s) as a worst case scenario[2]. A pulse repetition frequency of about 10 kHz is needed, as this will enable roughly 3 measurements per degree if spinning, and have more than enough to do a very stable single-point measurement. The chosen laser diode is limited in both pulse length and duty cycle to prevent it from taking damage due to overheating. The maximum allowed pulse duty cycle is 0.1 %, due to limitations of the laser diode. This means that if the whole period is $\frac{1}{f_{rep}} = 100\ \mu s$, then the allowed pulse is 100 ns with respect to laser diode. Given these values, a maximum allowed output power can be calculated using the IEC 60825. A laser can be harmful in several ways to the human body and the dangers varies from wavelength to wavelength. At $\lambda \approx 900\ nm$ the main danger is to the eyes. This is because the laser light can be focused by the eyes' own lens onto small spots on the retina where it can cause damage. Another reason this wavelength is very dangerous to the eyes is that it is not visible to the naked eye and will therefore not prompt any blink reflex. Given a laser strong enough, the skin may also be burnt. For a skin burn, a very high output power is needed, so only the eye-damage case will be considered. To be safe, three criteria must be met:

- MPE_{single} - The exposure from a single pulse must not exceed MPE.
- MPE_{avg} - The exposure for a pulse train of a certain exposure duration, T_{exp}, should not exceed MPE.
- MPE_{train} - The average exposure from a pulse train should not exceed MPE for a single pulse (MPE_{single}) corrected with the factor $N^{-1/4}$, where N is the number of pulses in the pulse train during the exposure time, T_{exp}.

All MPE used are calculated using "*Table 4 - MPE for eye regarding thermal and micro-mechanical retinal damage risk*" in IEC 60825.

The exposure time is set to between T_2 and $3 * 10^4\ s$, where $T_2 = 10\ s$ since the angular subtense, α is less than 1.5 mrad. α is assumed to be ≈ 0, since in a worst case, the victim is looking straight into the beam. Furthermore, the pupil size is estimated to a standard 7 mm diameter in a worst case scenario. First, the irradiance at the eye for a single pulse is calculated as shown in equation 10:

$$E_{e,single} = \frac{P_{out}}{\pi * (D/2)^2} \tag{10}$$

where $E_{e,single}$ is the irradiance for a single pulse at the cornea, P_{out} is the output power and D is the aperture diameter (the pupil). This is multiplied by the pulse time (t_p) and compared to MPE_{single}. MPE_{single} is calculated using equation 11 valid when $10^{-9} < t_p < 1.8 * 10^{-5}$.

$$MPE_{single} = 5 * 10^{-3} * C_4 * C_6 \tag{11}$$

where C_4 and C_6 are parameters determined by wavelength and α. $C_4 = 10^{0.002*(\lambda-700)}$ where λ is in nm and $C_6 = 1$ for $\alpha < 1.5\ mrad$. Given $\lambda = 905\ nm$, $C_4 = 2.57$. Finally, if $E_{e,single} * t_p < MPE_{single}$, it is considered safe with respect to single pulses.

[2]The correct way to do this is to assume an exposure time of a whole work day, which is defined as 8 hours. This seems very unreasonable, so a shorter, more reasonable time is used instead

The average exposure is determined in the same way, but using another formula for MPE_{avg} and another way of calculating the power. All these are calculated using equations 12-14.

$$MPE_{avg} = 10 * C_4 \quad (12)$$

$$P_{avg} = P_{out} * t_p * f_{rep} \quad (13)$$

$$E_{e,avg} = \frac{P_{avg}}{\pi * (D/2)^2} \quad (14)$$

where C_4 is the same as for the single pulse calculation, P_{avg} is the average output power and $E_{e,avg}$ is the average irradiance at the eye. Note that MPE_{avg} has the unit W/m^2, due to the long exposure time. It should therefore be compared to $E_{e,avg}$ directly, without multiplying it by t_p.

Finally, MPE_{train} is calculated from MPE_{single} using equation 15.

$$MPE_{train} = MPE_{single} * N^{-1/4} \quad (15)$$

where N is the number pulses in the pulse train. MPE_{train} is compared to $E_{e,single} * t_p$ in the same way as for MPE_{single}.

Using equations 10-15 and iterating the output power until all three criteria are met, it was determined that using the parameters $t_p = 100\ ns, f_{rep} = 10\ kHz$ and $T_{exp} = 30\ s$ the maximum allowable output power $P_{max} = 210\ mW$. If the detector is fast enough, a shorter pulse can be used, which means that a higher output power can be used. Therefore, to optimize output power, the pulse should be just long enough for the detector to be able to detect it, while taking into account the rise time of the laser diode and the limitations of the control hardware. After some testing, it was found that such very short rise times and pulse times could not be achieved reliably. The shortest pulse that could be achieved with good result was 60 ns. This would give a $P_{max} = 350\ mW$. Using some further tweaking, such as lowering the pulse length further and decreasing the repetition frequency, the output power can be increased even further. The final limit is the limitation of the laser diode. Since the chosen laser diode can output a maximum of 4 W at $t_p = 100\ ns, f_{rep} = 10\ kHz$, this laser diode should be more than enough.

2.1.4 Laser driver

A laser diode is current controlled. This means that the output power is controlled by current, rather than voltage. Once the current exceeds the threshold current the diode starts to emit light more or less linearly (output power varies linearly in relation to the current). Since laser diodes often operates at a high frequency, standard control techniques such as Pulse width modulation (PWM) cannot be used to control the output power. Furthermore, feedback from the light is often needed since the output efficiency (the amount of optical watts out per ampere in) decreases as the laser diode increases in temperature [14]. This is more important for a laser diodes operating in continuous mode than a laser diode operating in pulsed mode. Since the pulse is so short, the output power does not change much over time, since the laser has time to cool off between pulses. Therefore, it is for this project assumed that a certain current will always correspond to a certain output power. Even if it does not, it really does not matter, since it is not important that the output power is precise. The current is controlled through a programmable resistor and a pulse transistor. Since commercially available programmable resistors are both slow and has high resistance (the smallest in the range of 1 $k\Omega$), a custom solution was designed using 8 Metal-oxide-semiconductor field-effect transistors (MOSFETs) and resistors coupled in parallel as seen in figure 5.

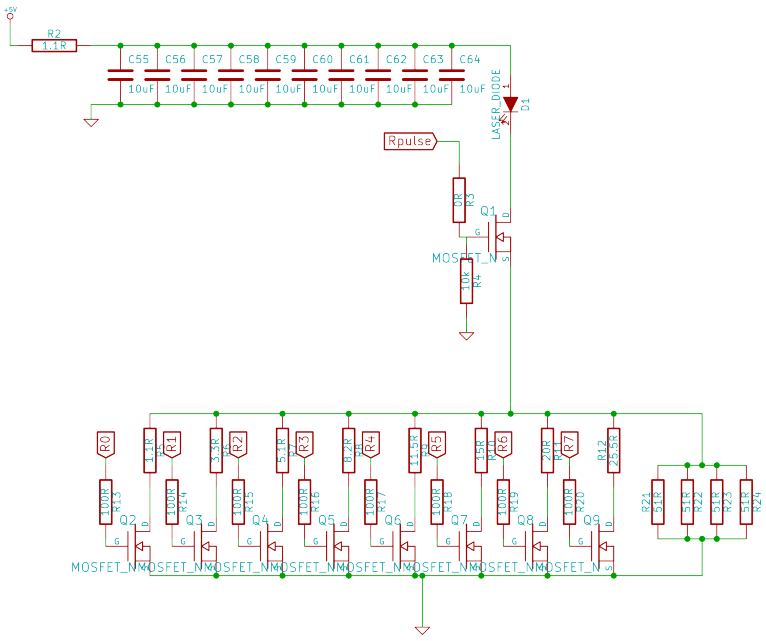

Figure 5: *The schematics of the laser driver circuit. At the top is a capacitor bank to provide the laser with lots of instant energy to allow for very fast and strong pulses. Below is a single MOSFET to control the pulse and 8 MOSFETs with resistors to control the output power. Finally, a threshold resistor is coupled in parallel with the rest of the programmable resistor to always achieve the smallest amount of current which makes the diode laser. The resistor values shown are calculated using the MATLAB script found in appendix 8.2.1.*

These 8 MOSFETs are set prior to the firing of a pulse, to ensure that these rise times do not affect the rise times of the laser. In parallel with the programmable resistor there is a set resistance to get ensure that the current passing through the diode is always just below the threshold current of the laser. The threshold resistance consists of several resistors, beacuse the power dissipation is too great to handle in a single resistor. These 8 resistors + the parallel threshold resistor gives a total of $2^8 = 256$ different power settings. The pulse itself is controlled by a single MOSFET of a faster type. A first design had these threshold resistors (controlled by a separate MOSFET) in parallel with the pulse MOSFET and the programmable resistor to keep the laser constantly just below threshold level to decrease rise times. This did not work very well, since this constant current drained the capacitor bank. It did not decrease the rise time noticeably. The resistance value corresponding to an output current can be calculated with the knowledge of the driving voltage, the voltage drop over the laser diode and Ohm's law as follows:

$$I = \frac{(U_{drive} - U_f)}{R} \tag{16}$$

where I is the current in A, U_{drive} is the driving voltage (which in this case is 5 V), U_f is the forward voltage drop of the laser diode and R is the resistance. The trouble here is that U_f changes with increasing current. This makes the calculation a little more tricky. The laser datasheet[12] specifies how U_f and output power (P_{out}) varies with I. The graph can be approximated by straight lines in two ranges: one are where I<1 A and one where I>1 A. However, in the case of I<1 A, it not reliable to look below I=0.3 A, since this is the threshold current of the laser. Therefore, the lower range will be valid only when 0.3 A<I<1 A. For both areas, equation 17 will specify the relation between the forward voltage and the current.

$$k_{IU} = \frac{U_2 - U_1}{I_2 - I_1} \ [V/A] \tag{17}$$

Where k_{IU} is the factor to relate the forward voltage to the current and U_1, I_1 forms a point in the graph. The first two points are found in the lower area: [2.2, 0.4] and [1.7, 0] gives $k_{IU,<1A} = 1.25$. The constant also needs to be added, which can be done using the equation for a straight line and inputting one of the points:

$$U = k_{IU} * I + m_{IU} \tag{18}$$

where m_{IU} is the offset. Using the first point [2.2, 0.4] $m_{IU,<1A} = 1.7$. Next, $k_{IU>1A}$ in the range where I>1 A can be determined by using the points [4, 6.5] and [3, 3]. This gives $k_{IU>1A} = 0.29$. The offset can also be determined in the same way as before, which gives $m_{IU,>1A} = 2.13$. P_{out} can be related to I using a straight line valid in the whole range where I>0.3 A.

$$k_{PI} = \frac{P_2 - P_1}{I_2 - I_1} \ [W/A] \tag{19}$$

Using the same method as before, the following points on the form [P,I] are selected: [0.8, 1] and [5, 6]. This gives $k_{PI} = 0.84$. Next, the offset is determined in the same way as before, which gives $m_{PI} \approx 0$. A more correct approximation of m_{PI} would be $-I_{th} * k_{pi} = -0.25$ since this is the output power if I = 0. Finally, combining equations 16-19 gives equation 20 which relates P_{out} to R:

$$R = \frac{U_{drive} - ((P_{out} - m_{PI})/k_{PI}) * k_{IU} + m_{IU})}{(P_{out} - m_{PI})/k_{PI}} \tag{20}$$

where k_{IU} and m_{IU} should be used with the range specific values. Also, to get which R to set given a specific P_{out}, equation 20 needs to be solved for P_{out}, which gives equation 21:

$$P_{out} = \frac{k_{PI} * (U_{drive} - m_{IU})}{R + k_{IU}} + m_{PI} \tag{21}$$

Since the resistance is set using 8 paralleled resistances, one more conversion is necessary before the power can be easily set using software. No closed-form equation was formed for this purpose. Instead, a look-up table was generated using a MATLAB-script (found in appendix 8.2.1). It maps a power output between in the range [0-255] to the eight resistors, whose configuration is represented by an 8-bit binary number. The resistances used were obtained using this script and are shown in figure 5. Due to the nature of paralleled resistors, this mapping is non-linear, which means that for high resistance, the resolution is low and vice versa for low resistance. However, due to the nature of the model, this is not true for the output power. As shown in figure 6, the transfer from programmed value to output power is more or less linear (but with a small discontinuity at the place where the model switches from low current to high current).

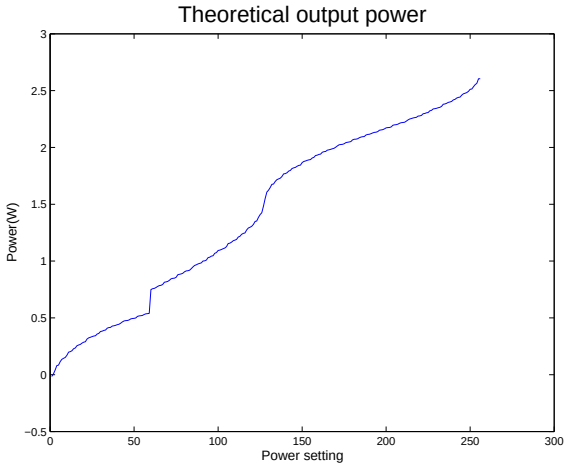

Figure 6: *Theoretical output power of the laser corresponding to the programmed value. As can be seen, its more or less linear, and not as non-linear as only the combined resistance.*

2.1.5 Laser optics

Laser diodes do not directly emit a laser beam, rather they emit light in an elliptical cone. This cone must be collimated into a beam to be useful as a laser beam. This can be done by using a collimation lens, which can be any lens placed at its focal distance in front of the diode. This collimation can be described mathematically by the equation 23[15] where y_1 and y_2 is the beam width before and after collimation respectively, θ_1 and θ_2 is the divergence angle of the beam and finally f is the focal length of the lens. It is also illustrated in figure 7.

$$y_2 = \theta_1 f \tag{22}$$

$$\theta_2 = y_1 / f \tag{23}$$

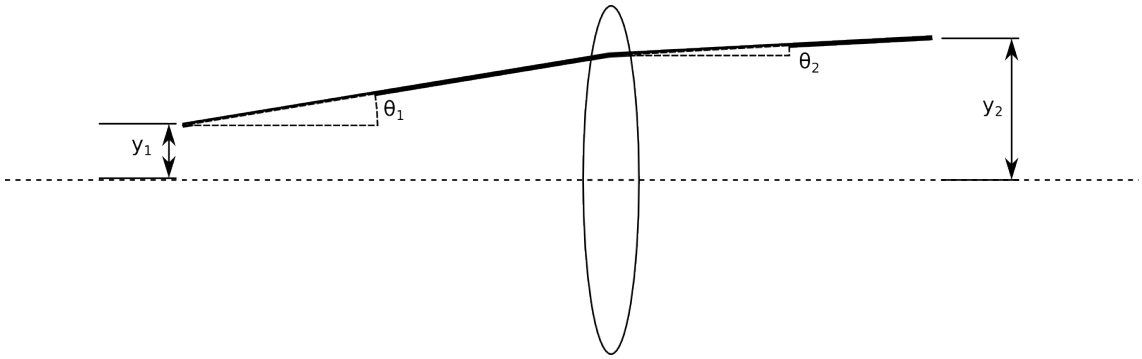

Figure 7: *Illustrates collimation of a laser beam. It shows how the divergence angle of the laser beam is decreased, while increasing the beam width.*

As can be seen in figure 7 any reduction in divergence angle will also have the added effect of increasing the beam width with the same factor. So a laser diode with a collimation lens with a focal length of 4 mm and a diode size in the 40 μm will increase the beam width by a factor of 100

and reduce the divergence angle by 100. As edge-emitting laser diodes emit light in an elliptical cone they have two different divergence angles. The chosen laser diode has divergence half-angles of $\theta_{\parallel} = 25$ degrees and $\theta_{\perp} = 9$ degrees in perpendicular axes[12]. This has been roughly verified as can be seen in the figure 8. The figure primarily illustrates the 25 degree divergence half-angle.

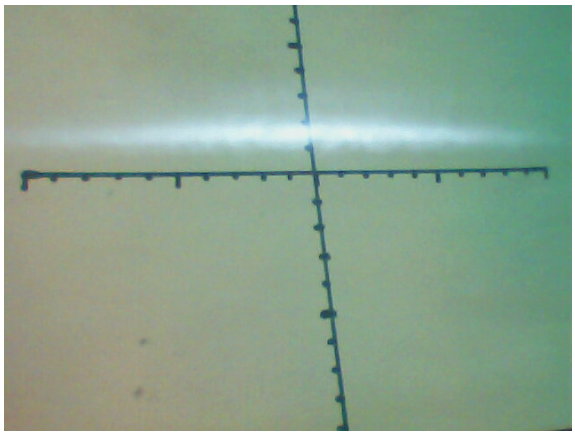

Figure 8: *A photo of the light emitted from the laser diode without any collimation lens. The light is projected onto a cm grid reference from a distance of 20 cm*

This ellipticity can be remedied by using two cylindrical lenses (lenses which only affect the light in one axis), one for each axis, each with a focal distance dependent on the divergence angle of that axis in sequence. It is also possible to use a lens with two cylindrical surfaces, one on each side, in perpendicular axis to perform the same task.

A single basic lens costs around €15-25, making using even a single lens expensive considering the budget of the project. Cylindrical lenses even more expensive, in the order of €35-45 each and two of those are needed to fully compensate for the elliptical beam. A custom-made combined lens would likely be several times the total budget of the entire project. The cost aspect makes it hard to include any compensation for the elliptical beam in the design. The idea was raised to use an existing lens scavenged from somewhere, as most cheap laser-pointers also uses the same type of laser diode. A laser pointer[16] was found that had a similar lens to what was needed. However, it is not a perfect fit. The lens from the laser pointer is adapted for the divergence angle of the laser diode from the laser pointer and it differs from the chosen laser diode. There is also a difference in wavelength. The lens's focal length and parameters in general are unknown. It should however be possible find a supplier of a more suitable lens at a reasonable price, since these are very common in laser pointers, and they are quite cheap. Since there was no time to find a lens with a perfect fit, the lens from the laser pointer was used and manually adjusted to allow the transmitter to produce a reasonably focused beam with reasonable beam width and divergence angle as can be seen in figure 9.

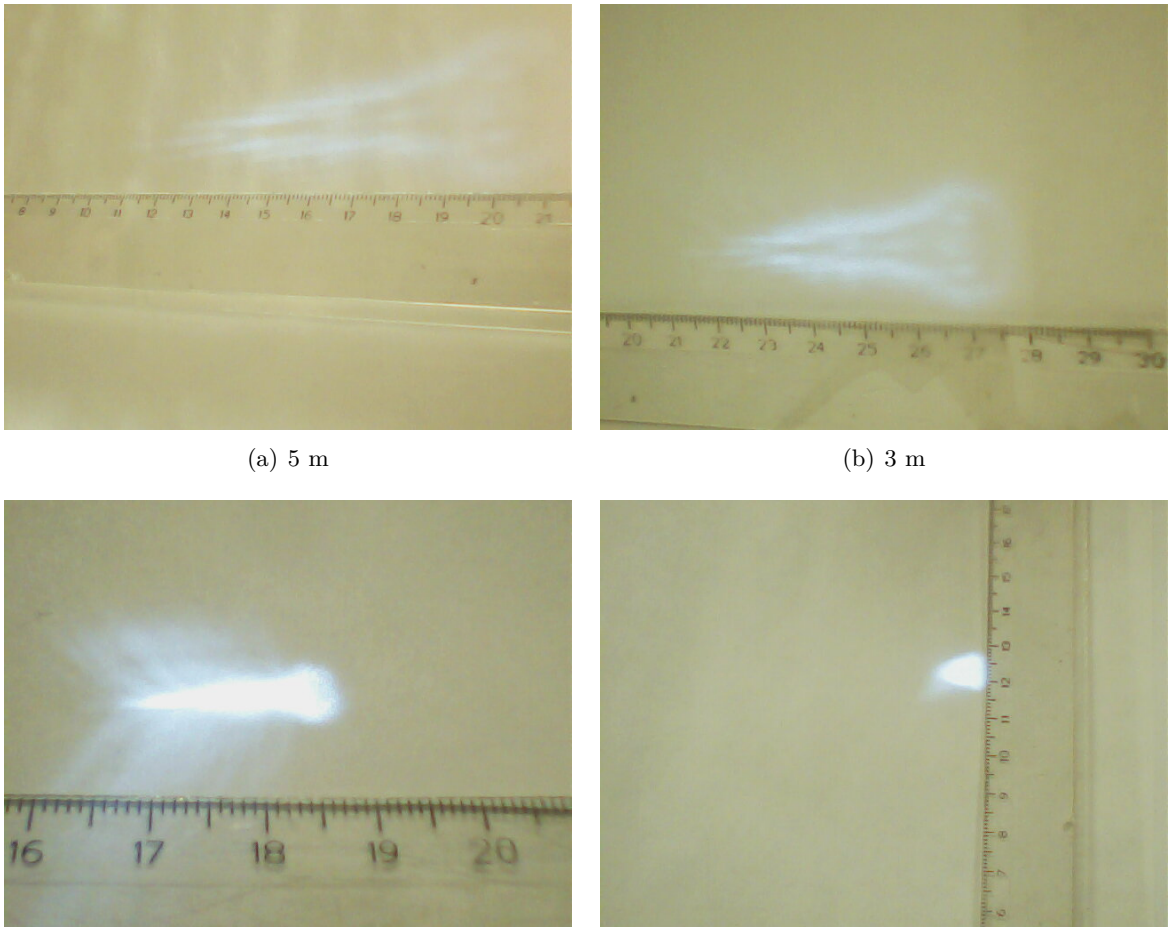

(a) 5 m

(b) 3 m

(c) 1 m

(d) 0.5 m

Figure 9: *Images of the reflected laser after the collimation lens at different distances. A metric ruler is used as size reference*

The divergence half-angle can easily be calculated based on the images in figure 9 using a right-angled triangle as shown in equation 24.

$$\theta = arctan((y/2)/L) \tag{24}$$

where θ is the divergence half-angle, y is the total observable width of the laser dot and L is the distance from the source. Using equation 24 and the images in figure 9, θ was found to be about 0.5°.

2.2 Receiver design

The receiver consists of four parts: an optical amplification assembly, a light detector, a signal amplifier and a sampling circuit (which measures time). The optical assembly gathers the light and focuses it into the detector. The detector receives the light and converts it into an electrical current that is amplified by the signal amplifier up to a level that the sampling circuit can detect. The design of these parts is discussed in sections 2.2.2 to 2.2.4. To be able to design the receiver, it is

necessary to first determine the amount of light the receiver is expected to receive. This is discussed in section 2.2.1.

2.2.1 Diffuse reflection

When the laser hits a non-reflective surface a portion of the beam will be absorbed into the material. However the remaining portion will be diffusely reflected, meaning the beam will be scattered and reflected in all directions. This scattering can be roughly modelled as the Lambertian model for diffuse reflections [17]. By approximating the light on the reflecting surface as a point, the light intensity emitting out from the surface can be modelled as a sphere where the diameter is the distance from the reflection at the surface to the receiver. The surface area of the sphere corresponds to the total light power reflected. From the surface with a certain area, a certain power is reflected. This power is then viewed at a solid angle based on the size of the viewing aperture and the distance from the reflecting surface and the receiver. The light intensity at the observer is changed based on the viewing angle, which is the main basis for the Lambertian model. This means that the power intensity of the light is given by equation 25

$$P_{in} = L_e * d\Omega_{obs} * A_{source} * cos(\theta) \tag{25}$$

where P_{in} is the light power intensity at the receiver, L_e is the radiance, $d\Omega_{obs}$ is the solid angle of the observer, A_{source} is the area of the reflection and θ is the angle of the observer (with respect to the neutral angle from the reflecting surface). The radiance can be calculated as show in equations 26 and 27

$$L_e = M_e/\pi \tag{26}$$
$$M_e = \rho * P_{out}/A_{source} \tag{27}$$

where, M_e is the radiant emittance from the reflection, ρ is the reflectance of the surface and P_{out} is the output power of the laser. Furthermore, the solid angle is defined as shown in equation 28

$$d\Omega = \frac{A_{det}}{L^2} \tag{28}$$

where L is the distance from the reflection to the receiver and $A_{det} = r_{det}^2 * \pi$ is the area of the receiver. Finally, equations 25-28 can be used to form equation 29 which relates P_{in} to P_{out}.

$$P_{in} = \frac{P_{out} * \rho * r_{det}^2 * \pi^2 * cos(\theta)}{L^2} \tag{29}$$

As shown in equation 29, the size of the laser spot does not matter. The only thing that the size of the laser spot affects is how hard it is to make the reflection hit the receiver and the uncertainty of the exact measurement point. Inserting values into equation 29 a factor between P_{out} and P_{in} can be calculated. ρ is very hard to predict, since different materials and colourings may have any reflectivity between 0 and 1. Good data on this was surprisingly hard to find, so a reflectance of something in between the extremes, say 0.5, is assumed. Since the distance is going to be much larger than the offset between the laser source and the center of the receiver, the angle θ is going to be very small, which means that $cos(\theta) \approx 1$ and can mostly be omitted. However, θ will be significant if the surface is angled from the LIDAR. This case will not be considered, to simplify the development process. Therefore, for the purpose of determining the input power, $cos(\theta)$ will be omitted. Using these values and L as the maximum measure distance ($L = L_{max} = 5$ m, as stated in table 1) the power intensity that hits the receiver can be reduced to as $P_{in} = P_{out} * r_{det}^2 * 0.20$.

Since the size of the detector will be small (a fast photo-detector has an area of about 1 mm^2) the input power to the electrical system will be very small. Therefore, an optical amplification is necessary before the photo-detector.

2.2.2 Receiver optics

Optics are needed to focus the returning light onto the detector. All the light gathered does not have to be focused on the detector all the time, just a sufficient amount to trigger a response from the detector. This means that at a short measurement distance the beams can energetic enough to satisfy that condition with only a smaller portion of the reflected light. The general set-up is illustrated in figure 10

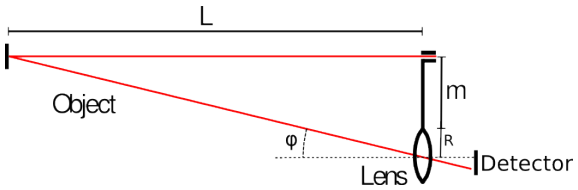

Figure 10: *An overview of the optical part of the receiver.*

The scenario is similar to the triangulation case discussed in section 1.1.2. In this case however, the goal is for the focused light to hit the same spot no matter the angle of the incoming light. This is so that the light can be maintained on the detector regardless of the angle of the incoming light. This is easier the smaller the angle of the incoming light is. If the angle is too great, the light will likely miss the detector altogether. This is what primarily defines the minimum measurement distance. The angle of the light is determined by the relative size between L and the distance between the laser and the center of the lens (m+R/2). Thus, the further away an object is the smaller the angle of the incoming light is. The angle can however be compensated for in several ways. For example tilting the lens towards the reflective surface is one method which would also reduce the maximum distance that can be measured. Another option for adjusting the minimum measurement distance would be to reduce the distance between the lens and the transmitter m or the lens diameter R.

More advanced set-ups include for example firing the laser through a hole in the detector lens, effectively removing most of the offset. When using this method one has to be careful not to cause a direct reflection inside of the lens. This however would be hard in terms of manufacturing, as it could also be very hard to isolate the outgoing beam from the lens, since only a small amount of stray light might trigger the sensor since the detector has to be very sensitive. Another method is to use a beam splitter, making it possible to eliminate the offset altogether by splitting the beam and using the same path both for transmitting and receiving light. One of them does however cost more than the entire budget[18], making them unreasonable for this application. Other than that, there would also be the downside of the splitting factor of the beam splitter reducing both output power and the amount of returned light. The reduction in output power could however be dealt with by simply increasing the output power until the intended power is reached on the other side of the beam splitter. The only realistic option considering the budget of this project is to use a single lens to focus the beam.

As illustrated in figure 10, the size of the lens will change the offset between the laser source and the center of the lens.

When choosing a lens many of the parameters of the system must be taken into account. In this case, the most important are the size of the detector, the minimum measurement distance and the offset between the laser source and the lens center. As shown in figure 9 the laser beam has a width. This means that each point in the surface area the laser hits will emit light in all directions, making it harder to model using ray tracing techniques since there will be an infinite number of points emitting light in an infinite number of directions. One way to model this system is in the same way as imaging of a camera is modelled, as can be seen in figure 11. y_1 in the figure should be considered as the offset of the laser source.

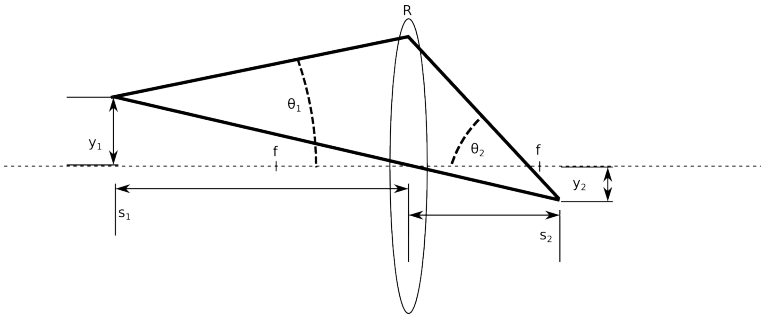

Figure 11: *How an object is imaged on the detector side through the lens.*

Equation 30 shows an approximation of the relationships between the important parameters using the imaging model. [15].

$$y_2 = \frac{y_1 * \theta_1}{\theta_2} = y_1 * \frac{R}{s_1} * \frac{f}{R} \tag{30}$$

This equation is derived from a property of lens systems called the optical invariant [19]. This means that in any optical system consisting of only lenses, the product of the image size and ray angle is always a constant, which is called the optical invariant as shown in equation 32. Combined with an approximation of θ_2 as $\theta_2 = R/f$, based on the the Gaussian lens formula [20] shown in equation 31 and the fact that if s_1 is very large, s_2 will be close to f.

$$\frac{1}{f} = \frac{1}{s_1} + \frac{1}{s_2} \tag{31}$$

$$y_2 * \theta_2 = y_1 * \theta_1 \tag{32}$$

Looking at equation 30 one can see that to focus on a small spot one would want to minimize y_2. This can be done by increasing s_1, which would mean moving away from the source. This is not possible since we want to measure the distance to the source, and therefore cannot control the s_1. It can also be done by reducing the lens size, reducing the received power quadratically due to the reduction of the receiving surface. However another thing to consider is that if the lens size is reduced, the offset between the laser and the lens center is reduced, decreasing the minimum measurement distance. A large lens will also force a longer focal length, due to the fact that it is difficult to create a lens with a shorter focus distance than radius. This will in turn limit how tightly the returning light can be focused.

Based on this, a lens candidate was chosen for further investigation and simulation. The lens chosen was the largest lens with the shortest focal distance possible satisfying the minimum measurement distance criteria defined in table 1. Using a lens this small may have limited the optical amplification, but it was necessary due to the size of the detector discussed in section 2.2.3 and the results shown in figure 12. The lens had 25 mm diameter, 25 mm focal length and cost €30 [21].

The thin lens equation [22] can give a rough estimation of where the focused light will hit and can be used to track the beam when it passes through key points. To be able to estimate the reflected power and its distribution at the focus requires a more exact method. Using the thick lens formula via the so called refraction matrix it is possible to track all beam paths through the system. This was done using a workbench in MATLAB [23] with the parameters of the real system as inputs, such as lens properties, placement and so on. By tracing a very large number of rays emitted from a random location from target surface with a random vector that intersects the lens a good simulation of the reflected light was obtained. The results for various distances can be seen in figure 12. The chosen placement of the detector (which is further discussed in section 2.2.3[3]) is shown by the red rectangle, which is 1x1 mm, and the white lines indicate the lens's optical axis and the entire image spans 5 mm.

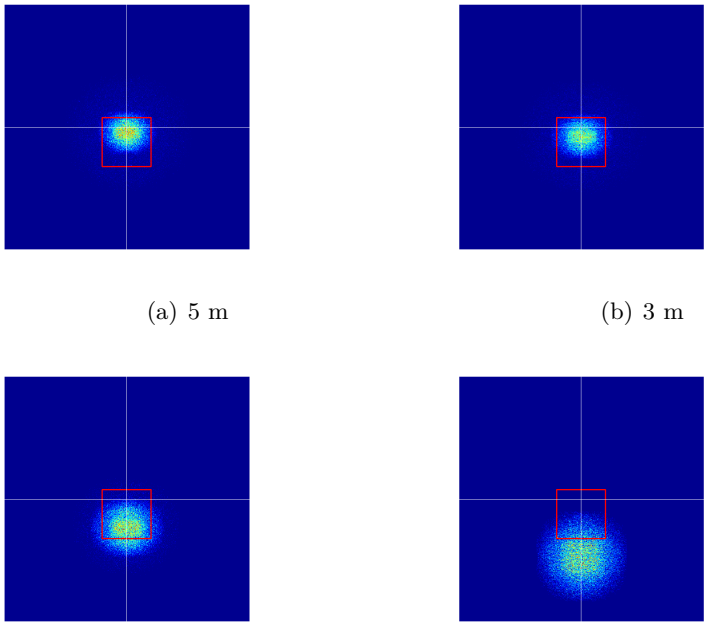

(a) 5 m (b) 3 m

(c) 1 m (d) 0.5 m

Figure 12: *MATLAB simulations of the reflected laser light after the focusing lens. These simulation were performed using an optical workbench for MATLAB [23]. Each of these images are generated using 100 000 rays where each ray has the following properties: a random point of origin (on the radiant surface), a random direction and that hits the lens.*

Using this simulation, a factor between the light that hits the lens and the light that is focused into

[3]Due to the development procedures not being linear, the detector was already more or less chosen during this stage of development. At least the detector size was assumed, based on the detector chosen and since it is a usual size for photo-detectors.

the detector can be estimated. With this information, an optimal placement of the detector can be determined to maximize the return signal over the whole measurement range. Using the decrease factor calculated from equation 29 the optical power that hits the lens can be calculated. Based on this and the results obtained form the simulations shown in figure 12 the worst case for light power that reach the photo-diode can be calculated. It was found that the worst case is at 5 m distance, which means that almost all light that hits the lens also hits the detector (given optimal placement). This means that the detector receives, given laser output power of 300 mW, $P_{in,det} = 9.25\ \mu W$.

2.2.3 Detector

The signal detector circuit consists of two main parts: a light detector and a signal amplifier. The detector has to be fast and be able to detect very weak signals. These two criteria contradict each other, as further discussed in this section. It is not possible to increase the speed and the signal amplitude at the same time (there is no free lunch). The approach will therefore be to find the fastest photo-detector available (at a reasonable price) and amplify the signal using the fastest amplifiers available.

Once again, components used for optical communication are considered. Photo-detectors are generally divided into two main areas: photo-diodes and photo-transistors. Photo-transistors are generally slower (rise times in the range of a couple of μs [24]) but do have some internal gain (as an inherent feature of being a transistor). However, with a signal shorter than 100 ns, these are not considered at all. This leaves photo-diodes. The main types of photo-diodes considered are p-n photo-diodes, PIN photo-diodes and Avalanche Photo-diode (APD)s. APDs are in theory well-suited for this application since they are extremely fast and have high internal signal gain. In practice they are not well suited mainly for two reasons: the price (they cost at least €50 a piece [25]) and the fact that they need high voltages to operate (in the range of 100-200 V [26]). PIN photo-diodes is just a special case of normal p-n photo-diodes, but faster, so the only type that will be further considered is PIN photo-diodes. First of all, the diode needs to be sensitive to the wavelength emitted by the laser. Since the laser light is of a standard wavelength (around 900 nm), a photo-diode to match that wavelength should be chosen. Furthermore, some photo-diodes have a shield to block out other wavelengths than the wanted one. This is of course desirable, since it will increase immunity towards random disturbances from surrounding light sources.

Photo-diode noise Next, the question "Will the photo-diode be able to detect the signal?" has to be answered. Noise in a circuit will come from many sources, such as the photo-diode itself, resistors, amplifiers etc. All these sources need to be weighed together to form a total noise. This is generally done as shown in equation 33[27].

$$E_{tot,rms} = sqrtE_{1r,ms}^2 + E_{2,rms}^2 + ...E_{n,rms}^2 \tag{33}$$

However, as a rule-of-thumb, if a noise source is much smaller than the largest, it is generally neglected.

A photo-diode can be used mainly in two modes in a detection circuit: Photovoltaic mode and Photoconductive mode. Since the photoconductive mode (also called reverse bias mode) offers much faster response times [28], this is the only mode considered. Further considerations include the noise level. Manufacturers often use a figure of merit called Detection Limit or Specific Detection (abbreviated as D^*). It is used to compare photo-diodes, but its usefulness is rather limited. Instead, what should be used is the Noise-equivalent power (NEP), which is the amount of light input power

needed to get an Signal-to-noise ratio (SNR) of 1. When a manufacturer specifies NEP, it is almost always normalized to 1 Hz. To get the SNR, the input power is compared to the NEP. The NEP should not only consist of the NEP for the photo-diode, but also the amplifier circuit (since the whole circuit will generate noise, and NEP of a photo-diode is the noise it generates). To choose the photo-diode, only the noise of the photo-diode and noise from any load resistor will need to be considered. To compare the input signal (at a certain power and with a certain pulse width) it needs to be normalized as well. First, the bandwidth of signal needs to be determined. The bandwidth of the signal is very hard to define in theory, since an ideal signal would be a strict square pulse, which would have infinite bandwidth. There are several ways to define the bandwidth. One way is to use the rise time using a rule-of-thumb as shown in equation 34 to define a bandwidth.[29, 30].

$$f_{c,3dB} \approx \frac{0.35}{t_r} \tag{34}$$

where t_r is the rise time of the system and $f_{c,3dB}$ is the 3dB cut off frequency usually used to define the bandwidth of a system [31]. Of course, the rise time has to be as small as possible to get a response as clear as possible, which means that an ideal signal would have an infinite bandwidth.

The other way is to approximate the pulse as a sine wave with a period of $2t_p$ and calculate a frequency from that, as shown in equation 35. This will give a lower limit of the bandwidth (the "fundamental frequency" so to speak).

$$f_{c,3dB} = \frac{1}{2 * t_p} \tag{35}$$

None of these methods are optimal to determine the bandwidth. The best way is to perform a Fourier Transform on the real signal to examine the frequency content. This however, is not feasible in the design phase of the project, so only theoretical calculations based on assumptions were performed as design aid. The bandwidth is calculated by the difference between the highest frequency content and the lowest as shown in equation 36.

$$\Delta f = f_{high} - f_{low} \tag{36}$$

where Δf is the bandwidth and f_{high} and f_{low} are the highest on lowest frequencies respectively.

The bandwidth is used to normalize the input power to form (P_{inNorm}) which is calculated in equation 37. Because the signal increases by the decreasing bandwidth and the noise by the root of the bandwidth, the square root of the bandwidth is used.

$$P_{inNorm} = \frac{P_{in}}{\sqrt{\Delta f}} \tag{37}$$

Finally, the SNR is calculated by comparing the P_{inNorm} to NEP, as in equation 38.

$$SNR = \frac{P_{inNorm}}{NEP} \tag{38}$$

SNR has to be at least one for the system to be able to detect the signal at all, but should of course be as high as possible.

Rise time The chosen operation of the photo-diode is, as mentioned before, reverse biased (photoconductive) mode. A photo-diode generates a current proportional to the incident light power. This current is then transformed into a voltage using a load resistor connected to ground, and the signal is read as the voltage drop over the resistor, which is, according to Ohm's law: U=R*I. This, together with the amplifier discussed in section 2.2.4, makes a so called transimpedance amplifier, which converts the current to a voltage to amplify it further. This is the usual approach for high-speed photo-diodes[32]. As seen clearly from Ohm's law, the amplitude of the output signal will increase with a larger load resistor. However, the rise time of the signal increases as the resistance increases. This is because the rise time of a photo-diode is determined by a time constant defined by three factors[28, 29, 33]:

t_{RC}: RC-constant, which is determined by the terminal capacitance and the series resistance (external resistance + internal resistance). It is determined by equation 39.

$$t_{RC} = 2.2 * C_t * R_l. \tag{39}$$

where C_t is the terminal capacitance and R_l is the load resistance. Included in C_t are also stray capacitances from the other components in the circuit, such as resistors, the amplifier and the Printed Circuit Board (PCB).

t_{Drift} : Carrier transit time in the depletion layer. It is proportional to the width of the distance of the depletion layer, which can be influenced by applying more reverse voltage.

t_{Diff} : Diffusion time, the time it takes for carriers generated outside of the depletion layer to diffuse.

These together form t_r as stated in equation 40

$$t_r = sqrt(t_{RC}^2 + t_{Drift}^2 + t_{Diff}^2) \tag{40}$$

It is once again shown that there is no free lunch (specifically from t_{RC}). It is impossible to get a strong and fast signal at the same time from the photo-diode and load resistor alone. The method chosen here is to optimize the rise time and to fix the small signal with an amplification circuit, where more energy can be put into the signal. Mainly, t_{RC} is going to be minimized since the other parameters are hard to influence. t_{Drift} can be influenced somewhat by increasing the reverse bias voltage, but is together with t_{Diff} mostly influenced by the design of the photo-diode itself. The main effort will be to use a small load resistor and to layout the board in such a way as to minimize stray capacitances. The load resistor could be chosen as 50 Ω, since this is a standard value for impedance in high speed communications. Usually, most detectors, amplifiers and other equipment are optimized for 50 Ω impedance, and it is important to make sure that the impedance is matched across the whole signal path to avoid reflections when the impedance changes. Furthermore, a higher reverse voltage will also decrease the capacitance, so a voltage as high as possible should be used here. This might be problematic, since this voltage would have to be supplied, which could be challenging.

Photo-diode selection The photo-diode chosen was the sfh203p from OSRAM[34]. This is a fast and cheap photo-diode used for optical communications. The detector size is 1x1 mm, which is a small detector. The top sensitivity is at $\lambda = 900\ nm$ and also features an optical shield with a rather narrow window (attenuates about half the amplitude at $\pm\Delta\lambda 100\ nm$ and more or less total attenuation at $\pm\Delta\lambda 150\ nm$). At this wavelength, the spectral sensitivity (which specifies the current generated by the photo-diode in relation to the incident light power) is $S_{\lambda=900\,nm} \approx 0.65$,

which is rather standard for silicon photo-diodes. The manufacturer specifies a rise time of 5 ns, which only applies under certain conditions which will never happen. Given some more information (such as information about t_{Drift} and t_{Diff}), the rise time could be calculated, but this information is not available, so the manufacturer specified value will be used as a lower bound. This rise time will correspond to the highest frequency of the signal from the photo-diode according to equation 34. This gives $t_{high} = 0.35/(5 * 10^{-9}) = 70\ MHz$. The lowest frequency from the photo-diode can be approximated using equation 35. This gives $t_{low} = 1/(2 * 100 * 10^{-9}) = 5\ MHz$. These two give, according to equation 36, $\Delta f = 70 - 5 = 65\ MHz$. This bandwidth is what the manufacturer specifies as the rise time of the photo-diode. However, the amplifier design (as discussed in section 2.2.4) is aimed at amplifying the signal quicker than the rise time of the photo-diode, thus creating a shorter rise time, which will effectively create a higher bandwidth. Furthermore, when it comes to noise, it is the bandwidth of the amplifiers that matters, since the noise is amplified at their bandwidth, disregarding the bandwidth of the signal.

As discussed in section 2.2.1, the optical power hitting the detector is $P_{in,det} = 9.25\ \mu W$ in the worst case (at the maximum distance). This means that current generated by the photo-diode will be $I_{diode} = P_{in,det} * S_{\lambda=900\ nm} = 6\ \mu A$. This current will generate a voltage over the load resistor according to Ohm's law: $U_{rl} = I_{diode} * Rl = 300\ \mu V$. Using the bandwidth and the input power, the SNR of the photo-diode itself can be calculated using equations 37 and 38 as shown in equation 42.

$$P_{in,norm} = \frac{9.25 * 10^{-6}}{\sqrt{6.5 * 10^{7}}} \approx 1.15 * 10^{-9} \tag{41}$$

$$SNR = \frac{1.15 * 10^{-9}}{2.9 * 10^{-14}} \approx 4.0 * 10^{4} \tag{42}$$

Equation 42 gives an SNR of 40 000, which is way more than sufficient. The noise from the photo-diode will not be considered any further.

The load resistor also generates noise dependant on the bandwidth. However, as mentioned before, it is the bandwidth of the amplifier that matters. This noise will therefore be calculated in section 2.2.4.

External light noise may present a problem to the detector. The amplitude of the source is unknown, but can be measured in the system (both during testing but also during operation). This noise source is countered by several measures: The photo-diode has a light-blocking shield (as mentioned before) which blocks most ambient light sources of incorrect wavelengths. Furthermore, since the system mainly works in high frequencies, it means that constant external light sources will not be trigger a signal, since the amplifier and conditional circuits only allows signals of the correct bandwidth. Finally, using a comparator (as discussed in section 2.2.4) will allow for dynamic setting of the trigger level to make sure that the system is robust against external light noise.

2.2.4 Signal amplifier

To amplify the returned signal is a difficult task. The very weak return signal has to be amplified greatly during a short time at a high frequency. This puts many difficult, if not maybe impossible, requirements on the amplifier. Two main methods were investigated to solve this problem: using Operational Amplifiers (OP-amps) and using RF-amplifiers.

OP-amps configured as a transimpedance amplifiers were the first type of amplifier method investigated. This amplifier converts the current through the receiver photo-diode into a voltage (as mentioned in section 2.2.3). The bandwidth of the signal is, as shown in section 2.2.3, very wide. It ranges from at least 10 MHz up to 1 GHz. Many operational amplifiers designed for frequencies in this region usually have only unity gain (a gain of 1 dB), which means they cannot actually amplify the signal. Because of this the selection of operational amplifiers is very limited. The selection criteria for the OP-amp was defined as "the fastest operational amplifier with gain at these high frequencies". Also a rise time of at most a couple of ns is necessary for a good measurement. The most important point is to get the same rise time for different input signal strengths. The signal has to be amplified from virtually 0 V up to 3.3 V before it can be used as an input to the timer circuit. Hence, the slew rate of the amplifier has to be sufficiently high. By using a comparator instead of an OP-amp, the slew rate can be increased substantially, since a comparator does not have a slew rate in the same sense as an operational amplifier.[4] Using a comparator at the end, it is not necessary to use operational amplifiers to amplify the signal all the way up to 3.3 V. It is really only sufficient to amplify the signal to a level where a comparator can distinguish it from noise. Another advantage using a comparator is the fact that a threshold level can be set. This means that the sensitivity of the detector circuit can be set dynamically. Comparators typically have an input offset voltage of 10 mV and an input bias current of 1 μA[36] (which will generate an input voltage based on the resistance in the circuit, according to Ohm's law). These constant offsets can be calibrated away by setting the reference threshold. This means that the signal in theory only needs to be amplified to get above the hysteresis (which is also usually around 10 mV) of the comparator. In practice, a signal much higher is preferred, due to both noise immunity and also since the comparator works better (faster and more predictable) the higher above the threshold the signal is. Therefore, the signal should be amplified as much as possible, even if about 100 mV would be sufficient.

The input signal generated by the photo-diode would have to be amplified to about 100 mV. As mentioned in section 2.2.3, the input signal is about 300 μV at its weakest. This means that amplification of a factor more than 300 (which is equal to about 50 dB gain) is needed before the comparator. The number of OP-amp stages needed for this is determined by the chosen OP-amp. If the gain of one OP-amp is not enough, several sequential OP-amps is required. The OP-amp should be connected as a non-inverting amplifier (since negative supply voltage should be avoided because of the extra work and components needed for this) and gain as much as it can. The gain loop should also have a capacitor in series to make sure that there is no DC-gain. The OP-amp chosen is an OP-amp with 12 dB gain. This means that 4 OP-amps are needed before the comparator. For full schematic, please refer to figure 31 in the appendix. The exact values of the resistors and capacitors was determined through testing.

OP-amp noise is something that was also considered. The SNR is never improved by simply amplifying the signal, since the noise is amplified equally. In fact, amplifiers worsen the SNR since all amplifiers introduce more noise. However, by constructing filters that match the wanted signal frequency, a large portion of noise can be filtered out. Only noise at the input of the first OP-amp will be considered, since the SNR won't be affected much by subsequent amplifiers, due to the gain of the OP-amp, which will make the input noise from the first amplifier dominant. An OP-amp has several input noise sources. First of all, there are constant current and voltage input offsets. These

[4] An OP-amp needs to be stable, since it needs to recreate the signal at a specific amplification. To achieve this OP-amps have limited slew rates for stability. A comparator on the other hand only needs to output a high or a low signal, which means that stability is not a requirement here. This means that a comparator can have more or less infinite slew rate in theory.[35]

can be dealt with by using high-pass filters (to block away any DC as mentioned before) and by adjusting the threshold at the end comparator. But there are also another types of noise sources to consider, such as random frequency dependent input noise. There is both a random input current and a random input voltage. These need to be weighed into the total noise level and compared to the signal level. From the data sheet of the OP-amp[37], it is obtained that the input voltage noise is $U_{ni} = 2.6\ nV/\sqrt{Hz}$. Since the OP-amp has a bandwidth of about 200 MHz, this frequency is used to determine the input voltage noise, according to equation 43. The noise caused by the resistors in the OP-amp feedback loop will be omitted to keep complexity of noise calculations down, since those calculations are not within the scope of this project.

$$v_{n,opv} = U_{ni} * \sqrt{\Delta f_{opamp}} = 2.6 * 10^{-9} * \sqrt{200 * 10^6} \approx 36.8\mu V \tag{43}$$

Next, the noise from the load resistor is on the photo-diode is calculated. Two kinds of noise will be considered: Johnson noise and shot noise. Both of these noises are generated mainly from the resistor.

Johnson noise is also called Thermal noise, or Nyquist-Johnson noise[38, 39]. It is generated by the electron movements in a resistor, creating heat which causes the resistance value to fluctuate. Since the mean amplitude of this noise is 0, the Root mean square (RMS) value of the noise is used. The RMS voltage is calculated as shown in equation 44.

$$v_{n,res} = \sqrt{4 * k_B * T * R * \Delta f} \tag{44}$$

where $v_{n,res}$ is the RMS voltage noise over the resistor, $k_B = 1.38 * 10^{-23}\ J/K$ is Boltzmanns constant, T is the temperature, R is the resistance and Δf is the bandwidth. $T = 300$ (room temperature 25 $°C \approx 300\ K$ is assumed), $R = 50\ \Omega$ and $\Delta f = 200\ MHz$ gives $v_{n,res} \approx 12.9\ \mu V$. This, compared to the signal voltage gives an SNR of about 23.

Shot noise is a random noise generated by current fluctuations. Current is electrons per time unit and electrons do not arrive in a steady stream, but rather randomly distributed (often modelled as a Poisson distribution[40]). The current noise is calculated as shown in equation 45:

$$I_n = \sqrt{2 * q_e * I_0 * \Delta f} \tag{45}$$

where I_n is the noise RMS amplitude, $q_e = 1.6 * 10^{-19}\ C$ is the elementary charge, I_0 is the current in the circuit (the current generated by the photo-diode in this case) and Δf is once again the frequency bandwidth. Using the current calculated before as $I_0 = I_{diode} = 6\ \mu A$ and $\Delta f = 200\ MHz$ gives $I_n \approx 19.6\ nA$, which is about 300 times smaller than I_{diode}. Therefore, shot noise will be neglected since the Johnson noise is much larger compared to the signal.

Both the noise generated by the OP-amp and the Johnson noise from the resistor are in the same region, so both need to be taken into account. Shot noise and noise from the photo-diode are not taken into account, since they are so much smaller. Furthermore, the other OP-amp input noise needs to be taken into account, namely the input noise current, which generates a voltage noise over the 50 ohm load resistor. Since this is a non-inverting amplifier, only the current generated at the non-inverting input will be considered. The current noise is $i_{n,opni} = 20\ pA/\sqrt{Hz}$ which converted to a voltage by knowledge of the resistor load can determine the input voltage noise using equation 46

$$v_{n,opi} = i_{n,opni} * \sqrt{\Delta f_{opamp}} * R_l = 20 * 10^{-12} * \sqrt{200 * 10^6} * 50 \approx 14.1\mu V \tag{46}$$

$v_{n,opi}$ is in the same order of magnitude as the other noises, so this needs to be weighed in as well.

Finally, the input noise to the first OP-amp is calculated using 33. The total RMS noise was found to be $v_{n,tot} = \sqrt{36.8^2 + 12.9^2 + 14.1^2}\ \mu V \approx 41.5\ \mu V$. Comparing to the signal voltage calculated in 2.2.3, the SNR was found to be ≈ 7.2. The SNR is degraded even further due to subsequent amplifiers, but this is hard to model without a complete circuit.

RF amplifiers were tested instead of the OP-amps at a late stage in the project. These amplifiers are different from OP-amps in the sense that they do not utilize a feedback loop in the same way. An OP-amp has to have a feedback loop from the output to the input, which is defined by the user, while a RF-amplifier is mainly a transistor with some bias circuits. Since OP-amps are designed to be stable, they have to be limited in speed (as mentioned before). An external feedback loop is also used to select the amount of gain. RF amplifiers on the other hand are a type of transistor amplifiers with very high bandwidth (up in the regions of several GHz) and gain of 20-30 dB at these bandwidths. They are often used in wireless applications where the signals are very weak and at a high frequency[41, 42]. Since a specific gain and stability is not needed, something that amplifies at a set gain and at a high wide bandwidth would be ideal. Since these have much higher bandwidth, rise times could be improved from the OP-amp solution, leading to less error in the measured time. These components are also typically very cheap and small, making them an even more attractive choice. There are many different kinds of RF amplifiers, and most of them require an RCL-filter, to optimize the amplifier for a specific frequency. There are however amplifiers which do not need this, since this circuit is included in the package. These are more easy to use, since less components are needed and should have a more optimal performance over a wider frequency range. Two candidates of RF-amplifiers were chosen: BGA2851[42] and BGA2818[43]. One of these operate at 5 V and the other at 3.3 V. For a schematic, please refer to figure 32 in the appendix.

RF amplifier noise should also be analysed. These generate noise in another way compared to OP-amps. If they generate any input noise similarly to OP-amps or resistors is unclear (the manufacturers don't specify it in the datasheet), but they specify something called a noise figure. A noise figure is a figure of merit describing the relationship between the SNR into an integrated circuit and the SNR out of it. noise figure is measured in dB and is related to the non-dB figure of merit noise factor as shown by equation 47.

$$NF = 10 * \log F \tag{47}$$

where NF is noise figure and F is noise factor. Using the noise figures of the chosen RF-amplifiers (3.5 dB[43] for the BGA2818 and 4 dB[42] for the BGA2851) and converting into F yields an SNR degrading of 2.2 and 2.5 respectively. This means when the signal passes through the amplifier, more than half of the SNR is lost. However, for cascaded amplifiers, the noise factor in each subsequent amplifier needs to be scaled down with the gain of the previous amplifiers. This is done using Friis formula for noise factor[44], as shown in equation 48.

$$F_{tot} = F_1 + \frac{F_2 - 1}{G_1} + \frac{F_3 - 1}{G_1 * G_2} + ... + \frac{F_n - 1}{G_1 G_2 ... G_{n-1}} \tag{48}$$

where F_n and G_n are the noise factors and power gain factors for amplifier stage n. Note that these figures are not in dB, but rather ratios. Using for example 2 amplifier stages, each with a $F = 2.2$, and a $G = 1000$ $(30dB)$, $F_{tot} \approx 2.2$ can be calculated. Since the gain is large, the noise from all amplifiers stages are neglected. This calculation does not include an additional noise sources in the subsequent stages, but since the gain is rather large, these can, like the noise factor

from these stages, be omitted. As these operate on a higher frequency, the noise from the resistor needs to be recalculated. These amplifiers have a bandwidth of 2.1 GHz, which means that noise should be calculated at this bandwidth. However, by using filters, the bandwidth can be lowered, decreasing the noise. Assuming a bandwidth of 1 GHz (corresponding to a rise time of 330 ps, which is about the needed timing resolution, as discussed in section 1.1.1), the Johnson and shot noises can be calculated using equations 44 and 45. Using these equations gives $v_{n,johnson} \approx 28.8\ \mu V$ and $v_{n,shot} = R * I_{n,shot} \approx 50 * 34.6 * 10^{-9} = 1.73\ \mu V$. Using equation 33 to calculate the total noise yields $v_{n,tot} = \sqrt{(28.8 * 10^{-6})^2 + (1.73 * 10^{-6})^2} \approx 28.9\ \mu V$. As seen, the shot noise has almost no effect. The SNR before the first amplifier can be calculated to $SNR = 300/28.9 \approx 10$. Finally, the SNR at the comparator can be calculated as $SNR_comp = SNR/F = 10/2.2 \approx 4.5$. This is probably doable, but more SNR is of course desirable. This can be achieved by using another amplifier with lower noise factor or using more filtering.

Avalanche transistors present an alternative approach. They work in the same way as APDs to achieve very short rise times, however at the same cost of high voltage (again in the range of 100-200 V), availability and high cost. Therefore, these will not be further investigated.

2.3 Time measurement

As mentioned before, time of flight measurements are not possible without something that can measure time very precisely. There are several ways to solve this problem, but the easiest way is to use a dedicated integrated circuit. These circuits are uncommon to get off-the-shelf, since it's easier for a large company to use an ASIC for this purpose, which may also contain a signal amplifier. The simplest solution is to use a fast microcontroller timer to measure time. However, to achieve a resolution of 334 ps, the clock frequency F_{clk} would have to be according to equation 49

$$F_{clk} = \frac{1}{334 * 10^{-12}} \approx 3 * 10^{12}[Hz] = 3GHz \tag{49}$$

3 GHz is a very high frequency and no microcontrollers (seldom even real processors) use this high a clock frequency. So, this solution is not feasible at all. The fastest microcontrollers today have timers that go up to 256 MHz[45], which is more than 10 times below the frequency needed to fulfil the requirement.

Another method for measuring times could be a constant current source charging a capacitor during the time the light is travelling. When the light is received, the charging stops and the charge in the capacitor correspond to the time. The good thing with this is that it is probably cheaper than an integrated circuit and the resolution is given by how exact the charge in the capacitor can be measured (which often is at rather high resolution). The downside is that it would need to be designed and tested, which is generally very hard, since it involves high speed and precision electronics. PIC microcontrollers from Microchip has such a module built-in (called a CTMU). It was hard to find the exact resolution for this, but most sources claim below nanosecond resolution [6], which probably means hundreds of ps, and this solution could therefore be feasible. The price of these microcontrollers is generally low, so it would definitely fit within the budget.

The best solution is to use an integrated circuit specifically designed for measuring short times. These are very uncommon on the consumer market. Texas Instruments manufactures a TMU circuit with a precision of about 13 ps. Unfortunately, it is rather expensive (a price at about €120), which is over our budget[5]. Acam manufactures TDC-circuits [46] in several variants. The one best suited for this application was the TDC-GP21. It can measure time with a 45 ps resolution (22 ps if

using only one of the two channels). By using oversampling techniques, a higher resolution can be obtained, as long as the process has a randomly distributed error. Even without oversampling, the resolution is several times the needed resolution (of 334 ps). At a price of about €10 it is a given component in the system. This specific TDC measures time by letting a signal pass through a series of inverters with a very known propagation delay. When a stop signal is generated, the position of the signal is saved and a time can be calculated from this [47].

2.4 Microcontroller

The microcontroller is the controlling and supervising part of the system and it also serves as an interface to the system from external units using the LIDAR. To ease with development a microcontroller available on a cheap development board was selected, an STM32F407VG [48] mounted on an STM32F4Discovery[49]. It is one of the fastest and most powerful microcontrollers available at the time of writing. It operates at a frequency of up to 168 MHz, incorporates all the necessary peripherals such as ADC, Digital-to-Analog Converter (DAC), many hardware timers and various communication interfaces such as USB, UART, SPI and I2C.

To be able to flexibly set the things such as the laser pulse length, the timing between start and laser pulses and so on it is best if this could be done in software internally in the microcontroller. Since the laser pulse is very fast, it is necessary that the microcontroller clock speed is enough to allow for enough resolution. Also, using the microcontroller clock to generate the pulse means that the pulse length can only be in multiples of the clock frequency. However, software cannot be used directly to generate pulses, since the core is unpredictable for these time frames, probably due to advanced functions such as instruction pipelines and so on. Therefore, the internal hardware times should instead be used. These are easily programmable and synchronizable to generate very precise pulses (at a resolution of about 6 ns, based on the microcontroller clock frequency of 168 MHz). The DAC is used to set a voltage level for the comparator part of the amplification circuit that defines the threshold for which values are regarded as noise and which are real values. The ADC is considered as a way to directly measure the voltage level of the input signal, but it is uncertain if it can be used since it might interfere with the signal itself. The circuit board is therefore designed to allow for easy disconnection of the ADC. The interface with the TDC is via Serial Peripheral Interface (SPI)[47], which can be used at high speed since it is a synchronous protocol[50]. The rest of the interfaces are to be used mostly to interface a user, however primarily UART will be used during development since it is a protocol widely used to interface with subsystems on many robots and it is one of the easiest to work with. One could also think to use SPI, to handle the possibly high data rate from the LIDAR.

2.5 Hardware design

To hold everything in place, some hardware assembly is needed. The hardware design was based on the criteria of the other parts, in particular the optical requirements. The hardware should incorporate all parts of the system: the laser diode and transmitter lens assembly, the receiver diode and receiver lens assembly and some place to mount the PCBs. Furthermore, all optical assemblies should be adjustable to calibrate for any manufacturing errors. The transmitter lens needs to be adjustable in relation to the laser diode in the the beam direction and it should be possible to aim the whole transmitter assembly in the other directions, which means that the laser beam should be adjustable to fire a beam in any direction (within a certain limit of course). More

or less the same thing goes for the receiver assembly. The receiver lens should be adjustable in relation to the receiver diode, both the beam direction (z direction) and in the other two directions (x- and y directions). The design freedom for both these cases is to choose whether to move the lens or the transmitter/detector diode.

2.6 Scanning

Scanning has only been briefly investigated since it was removed from the specification at an early stage. An early concept image is shown in figure 13. The main reason why it was removed was that it would take too much time. Another reason was to remove any complications stemming from integrating scanning into the system. As it is now the system has the measurement frequency to support scanning measurements but scanning is not integrated into the system. If the system specifications are met then scanning can be realized rather easily by rotating the entire system and using inductive or slip connectors to interface with the system.

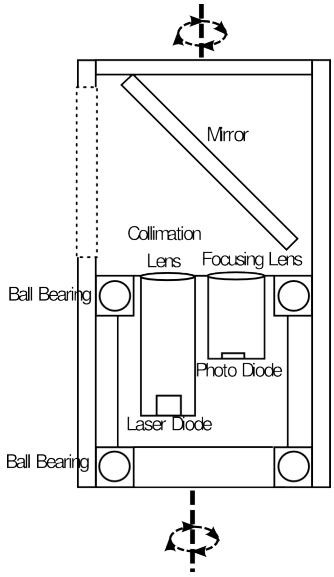

Figure 13: *Conceptual image of a scanning LIDAR*

3 Testing equipment

To perform tests to verify the functionality of the device, certain testing equipment was needed. At high frequencies are used in this project, it is important that the testing equipment is suitable for these frequencies and is used correctly.

3.1 Oscilloscope

An oscilloscope is an invaluable tool for testing electronics. Using this it is possible to observe the behaviour of the high-speed signal and properties such as amplitude, rise- and fall times and durations. For this project, two different kinds of oscilloscopes were used: Rigol DS1052E 50 MHz, 1 GSa/s and Tektronix TDS3032B 300 MHz, 2.5 GSa/s. These oscilloscopes are really a little too slow for measuring these signals (especially the Rigol), but those were readily available and enough

for coarse measurements. Generally, x10-mode was used on the oscilloscope probes, to make sure that the circuit measured was affected as little as possible from the measuring equipment. Both of these oscilloscopes can save the data on an external medium. The Tektronix oscilloscope was old, so it could only save on diskettes, making it harder to sample data from it.

3.2 IR camera

One of the hardest things when researching IR equipment is to observe the IR. One way to do this is to use a cell phone camera, since they usually don't have an IR filter. However, cell phone cameras are not of the best quality (they don't usually have any optics at all for instance) so a better camera is preferred. One can easily modify a normal webcam to be IR sensitive by removing the IR-blocking filter on the image sensor. Then it can be connected to any PC and IR can be seen. This type of modified webcam was used throughout the project.

3.3 Light power meter

A light power meter was used to measure the optical output power of the laser. It consists of a well calibrated photo-diode, PIN-10D[51], and a battery. By connecting it to an oscilloscope, the optical power can be measured. There are however two major drawbacks with this specific sensor: First, the sensor area is very large, which makes it very slow. Secondly, the lasers optical output power is rather high, which means that to match this output power, the photo-diode would have to match this and output a high of current. The photo-diode has a spectral sensitivity ($S_{\lambda=905nm}$) of 0.65 A/W, which means that for each watt in optical input power, it outputs 0.65 A. Given an input power of more than 1 W, it needs to output more than 0.65 A, which is too much for this (and most) photo-diodes. This can be solved by using an optical filter to limit the input power by a known factor.

4 Results

This section consists of two main parts: first a description of the subsystems in the LIDAR (found in sections 4.1-4.3.2) and second a verification of each subsystem (found in section 4.4).

4.1 Electrical design

The electrical system consists of two PCBs: a main PCB and a detector PCB. Both of them are designed using KiCad and incorporates all electrical components according to their specifications. All schematics can be found in appendix 8.1.

4.1.1 Main PCB

The main PCB contains the microcontroller (STM32f407VG), the TDC (TDC-GP21) and the laser driver. Furthermore, it contains all components needed around these main components, which are mostly capacitors, resistors, LEDs and pin headers. The PCB also has expansions for future development, such as a USB-port and a socket for an SD-card. The large amount of capacitors is necessary to keep the voltage on a very stable level because the TDC needs a very stable voltage to

perform the high-speed measurements accurately. There are 4 voltage systems on this board: first two 3.3 V systems, where one supplies the TDC core and the other supplies the rest of the logic (including the microcontroller). Second, two 5 V systems, where one is the voltage used to drive the laser and one is used to drive the detector electronics. It could be potentially bad if these 5 V systems used the same source, since the laser consumes current at very high pulses, which might interfere with the very sensitive detector and amplifier electronics. Photographs of the the main PCB with most components mounted can be seen in figure 14.

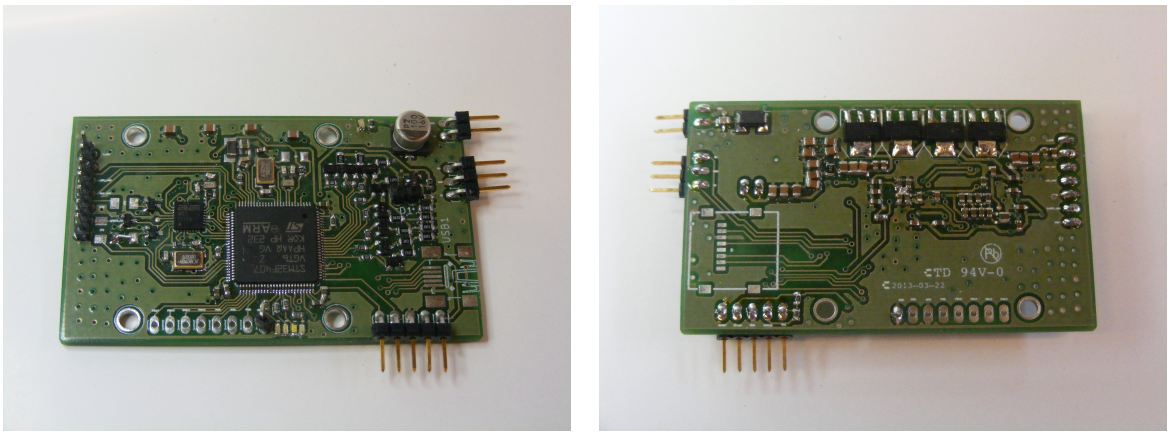

(a) Front (b) Back

Figure 14: *A photo of the main PCB*

4.1.2 Detector PCB

As discussed in section 2.2.4, there were two different approaches to the detector PCB: one with OP-amps and one with RF-amplifiers.

OP-amp solution To ensure minimum interference from other radio-sources (since these amplifiers operate on high frequencies) and keep noise levels down, all high speed electronics were encapsulated in a grounded copper shield as can be seen in figure 15(b). For testing purposes, measurement points are located on the board and has small "antennas" sticking out to the top side. These may act as antennas on frequencies the amplifiers work on, but no large weight was put on minimizing this potential noise source, since the antennas are rather short and will be removed when the system has been verified. The PCB in figure 15 is the latest OP-amp-based amplifier design. As for the circuit design it is available in appendix, figure 31.

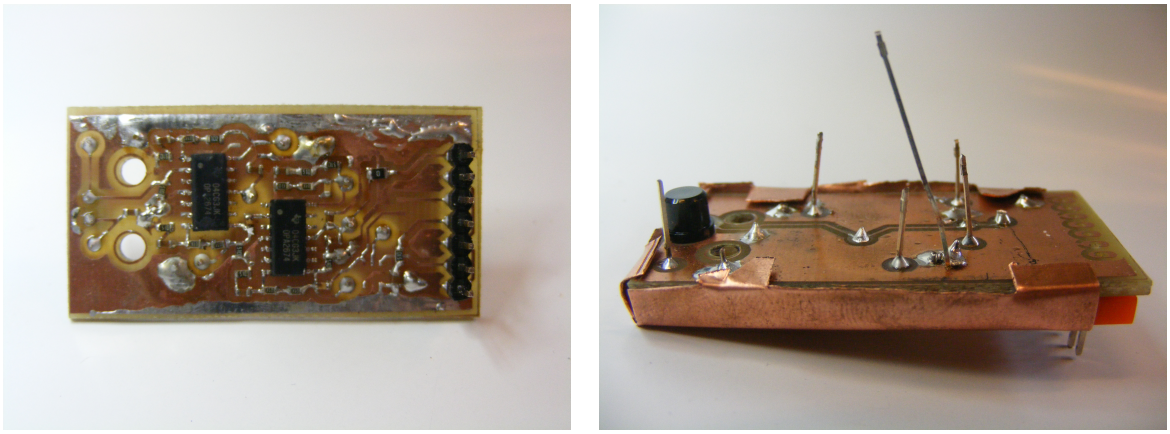

(a) Unshielded (b) With shield

Figure 15: *Photos of the latest OP-amplifier-based PCB design with and without shielding*

RF-amplifier solution The amplifier boards have been developed iteratively and the PCBs used at the end of the project does, as mentioned before, not use OP-amps at all, but rather RF-amplifiers. These are according to the specifications better suited for the system as pointed out in 2.2.4. These boards had not been sufficiently tested at the end of the project, so they are still heavily unfinished, but the last experimental PCB is shown in figure 16.

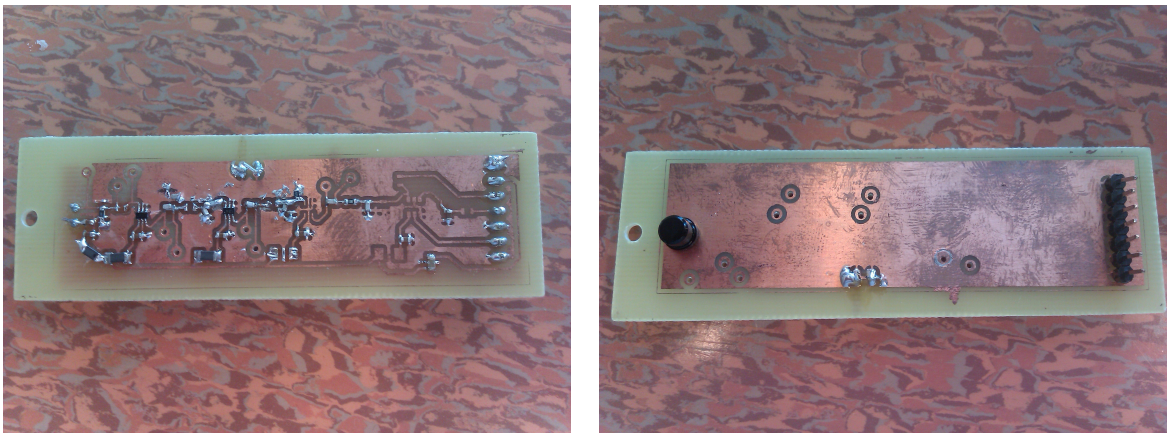

(a) Back (b) Front

Figure 16: *Photos of the latest RF-amplifier-based PCB front and back*

It is mainly a breakout-board to experiment on to test filter parameters. It is also an experiment in terms of signal routing to reduce noise. As this is a basic test version there is no shielding used besides the ground plane. The schematic is available in the appendix, figure 32.

4.2 Software design

The far most significant software is the C code for the microcontroller that controls the system. This code primarily controls the laser pulse and output power (through the "programmable resistor"

discussed in section 2.1.4) and interfaces with the TDC. The highly time-critical parts, such as the length of the laser pulse, the timings between the start pulse to the TDC, the laser pulse and the stop pulse used for testing are controlled by synchronized hardware timers. The stop pulse is only directly controlled by the microcontroller when testing the TDC. A UART interface that enables these settings to be changed without reprogramming the microcontroller was implemented. Aside from this no other interfaces besides a few status LEDs were implemented. As mentioned in section 4.1.1 there is hardware support to expand the interfaces to USB and SD-card, but this was not deemed necessary during development. The C-program also contains some code regarding the amplifier threshold, both for measuring and estimating the voltage level via the ADC as well as setting the voltage reference threshold of the amplifier comparator via a DAC as described in section 2.4. This was however never actually used. All functions use the hardware peripherals in the microcontroller when applicable to make sure the load is minimal for the microcontroller to more easily enable heavy data processing and management later on.

A short python script was developed to enable a Unix based pc to more easily interface with the microcontroller through a USB-to-UART converter. It was primarily used when performing large sampling series on the TDC.

Furthermore, as mentioned throughout the report, MATLAB was used during the development, both to handle post-processing of collected data, and to test out various parameters of components.

4.3 Hardware design

As described in section 2.5, the hardware is simply there to keep the chosen components (lenses, detectors, laser diode and so on) in the correct place in relation to each other. During the project, two different designs were designed and manufactured.

4.3.1 First design

The first design was to be used as an evaluation for different components. It was also designed for use with standard optical tables and setups. The design has the transmitter and receiver as separate parts to allow for maximum flexibility during tests and to ensure compatibility with existing optical equipment in the laboratory. Both the receiver and transmitter are based on two quadratic blocks each; one for the component and one for the angle correction. The blocks are made from polyacetal because it is a very easily processable material, it does not bend and it is rather strong [52]. All parts are either CNC milled or manually lathed. Images can be seen in figure 17.

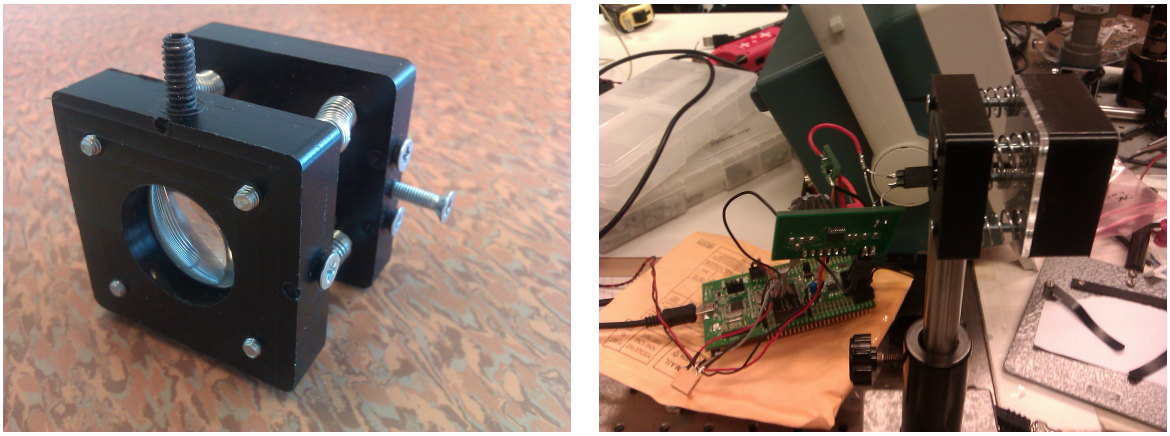

(a) Receiver (b) Transmitter

Figure 17: *Photos of the first version of the hardware. No real computer models were made of this design. Note that the transmitter prototype was lost, so no better image of it can be produced.*

The transmitter has a small lens holder integrated in the same block as the laser diode. It is threaded on the outside and the lens is spring loaded against the laser diode. The height is adjusted by screwing the holder up and down in the threaded hole surrounding the laser diode. The angle is adjusted by 4 screws connecting the laser diode block to the holder block. All screws are spring loaded to ensure stability by keeping everything under tension. The holder block is then screwed onto standard holder for optics, to enable it to be easily used on optical tables.

The receiver has the same structure as the transmitter, except that the detector diode and the detector lens are located on separate blocks. The front block contains the lens and the back block contains the detector diode. By turning the screws, the detector lens can be moved further away, closer or tilted in relation to the detector. The amplifier electronics are located behind the detector diode.

4.3.2 Second design

The second design is a more integrated solution, where the transmitter and receiver are located on the same unit. The troubles with the first design was that it was hard to position the transmitter and receiver in a good relation to each other, but most of all because they could not be put as close to each other as would have been necessary since the shortest detectable distance is increased with the distance between detector lens center and laser diode (as discussed in section 2.2.2). The second design allows the lens center and laser diode to be put closer to each other, but at the expense of some flexibility compared to the first design. This design contains the same main parts as the first design: one transmitter and one detector part. The main differences are that the transmitter and detector are mounted on the same piece and the way they are adjusted. The physical prototype and the computer model can be seen in figure 18.

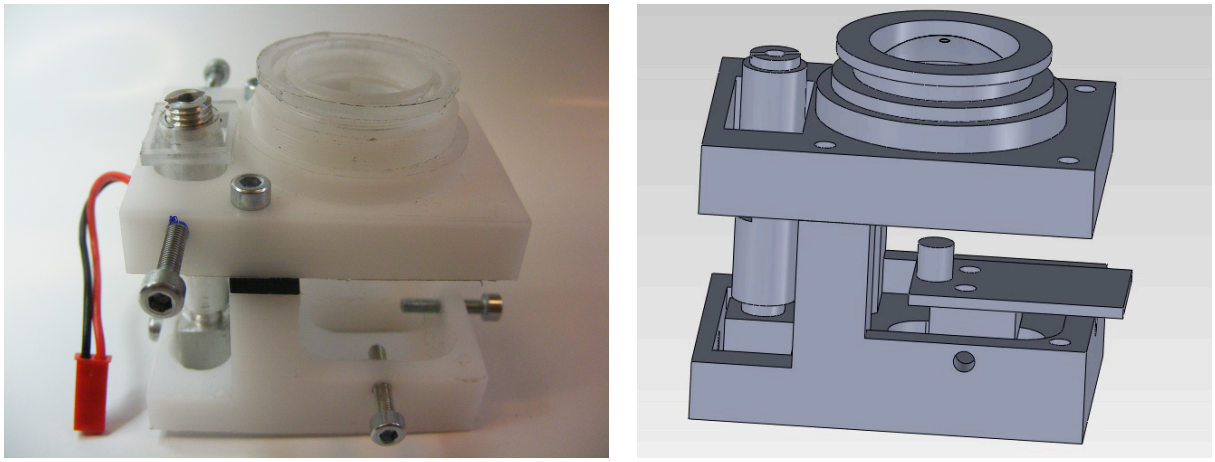

(a) Physical prototype (b) Computer model

Figure 18: *A photograph of the assembled hardware without any PCBs as well as the computer model it is based on.*

The transmitter design was influenced by a cannon. Since the laser diode tilts up to 5 degrees [12] from its own axis within the package (with respect to the bottom of the package) it must be possible to tilt the laser diode. This is achieved through a solution which allows the user to aim the laser diode in almost any direction by rotating it around its own axis and tilting it back and forth (analogue to a polar coordinate system). The laser diode is located in a tube, which is screwed onto a tiltable holder. Inside the tube, the lens is held by the the same lens holder solution used in the first design. The tilting is controlled by two screws and a spring. This is to keep the tilt at a steady angle and to be able to tilt it with precision.

The receiver also takes a different approach than the first design. Instead of changing the angle of the lens in relation to the detector diode, the detector diode is moved in the focal plane of the lens and the lens can be moved up and down to adjust the position of the focal plane. The lens is positioned in a holder with threads on the outside. By fastening the lens with a bolt with tight threads, the bolt can be used as holder when adjusting the focus. The detector diode is mounted on the amplifier PCB, to ensure shortest possible signal paths when the signal is weak. The PCB is mounted on a small block located in a pocket below the lens. The block can be adjusted within the bounds of this pocket with screws and springs from the sides. This block is kept pressed against the bottom of the pocket with a screw using a large washer on the other side.

4.4 Subsystem verification

Before testing the whole system together, each subsystem was verified separately. This section presents the results of these tests.

4.4.1 Transmitter

Three parameters need to be verified for the laser: output power, rise time and pulse length. Determining these three things is quite hard, but could be done using a calibrated photo-diode.

However, as discussed in section 3.3, the equipment available was ill suited to measure some of these parameters.

Output power was the first parameter measured. The light power meter was used to determine the output power of the laser, by focusing the light on the large detector and attenuate it with optical filters. The output signal was measured using the Tektronix oscilloscope over 50 Ω impedance which resulted in a voltage difference. The resulting signals for three different output powers are shown in figure 19.

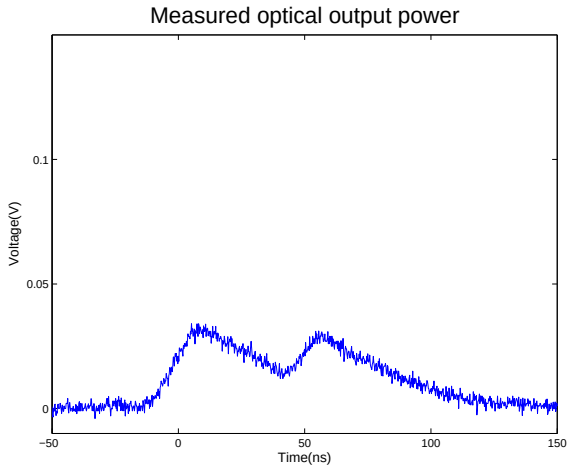

(a) Power setting 10

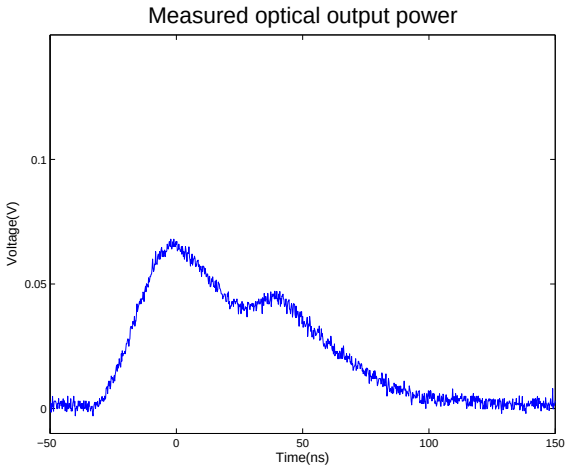

(b) Power setting 50

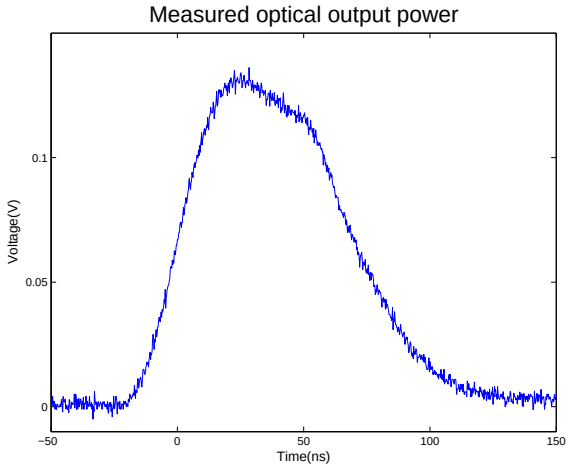

(c) Power setting 100

Figure 19: *Laser light pulses measured using the light power meter. The power setting is a programmed value corresponding to the output power as explained in section 2.1.4. Due to the configuration of the photo diode, the real signal was inverted. For ease of comparison, the curves are inverted (because the power should not be negative).*

The maximum output power was sampled at the highest voltage peak, and the resulting output

power could be calculated using equation 50

$$P_{out} = \frac{U_{peak}}{T * R * S_{LPM,\lambda=905nm}} \tag{50}$$

where U_{peak} is the highest voltage peak, T is the transmittance of the filter, $R = 50\ \Omega$ is the load resistance and $S_{LPM,\lambda=905nm}$ is the photo-diodes spectral sensitivity at the wavelength 905 nm. Using the values $T = 0.045$ and $S_{LPM,\lambda=905nm} = 0.65$, a conversion factor ($k = 0.68$) could be calculated to relate P_{out} to U_{peak}. This measurement was performed for several output settings and compared to the theoretical output power (based on the model discussed in section 2.1.4). The results are shown in figure 20

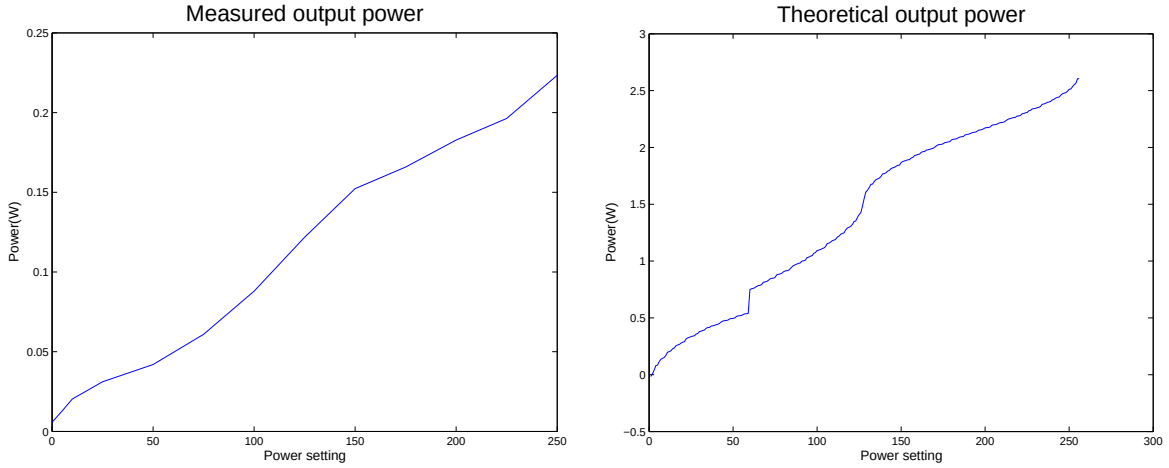

(a) Measured power

(b) Theoretical power

Figure 20: *Comparison between theoretical and measured optical output power. It can be seen that they follow the same general shape, but the measured output is smaller by about a factor of a little more than 10*

As can be seen from figure 20 the measured output and the theoretical output are very similar in shape. However, the measured output is much smaller. This can be explained by the placement of the collimation lens. To get a good shape on the output light, the lens had to be placed far away from the laser diode. Due to this, most of the output power from the laser diode has diverged before it hits the lens. Furthermore, the light is clipped due to an aperture hole in the lens holder. The lens is located about 10 mm from the laser diode. The aperture hole is 3 mm in diameter. Given the divergence angles discussed in section 2.1.5 the beam can be approximated as a rectangle at the lens. The relation between the optical output power emitting from the lens is the same as the relation between the area of the rectangle and the aperture. The rectangle can be calculated using trigonometric relationships and was found to be about 10x1 mm = 10 mm^2. The aperture area is 7 mm^2, but the laser line does not overlap the aperture in fully. Therefore, the overlapping part will be approximated using a rectangle with size 3x1 mm = 3 mm^2. The power reduction factor can therefore be approximated to 0.3 based on the geometry. However, there are other factors which may reduce the power output such as the lens not being optimal for this wavelength, and might absorb some power or the laser diode might be tilted in relation to the lens. Therefore, the observed power ratio of slightly above 10 seems reasonable. This output power reduction is not good, since it will make the system more inefficient. However, given the power reduction, it is possible to increase the set output on the laser diode and still be eye-safe. Ideally, a better transmitter setup should be developed instead, since it is never good to waste a lot of energy.

Rise time was determined next. The rise time can be determined by using several methods and choosing the shortest result, which gives an upper bound of the rise time, since the measuring equipment might add some rise time (the actual laser rise time cannot be slower than what is shown in the oscilloscope). The first solution is to check the rise time of the voltage drop of the laser diode. This was very hard to do, most probably due to the very fast and powerful dynamics of the laser. Furthermore, the laser is mounted on a cable, which acts as an inductance and an antenna, perverting the signal and causing oscillations. This method is not the optimal since the rise time of the voltage drop not necessarily corresponds to the light emitted from the laser. It is however assumed that this is the case, since it consists with what is presented in the data sheet [12]. The measurement result presented in figure 21 shows that the voltage drop over the laser diode had a rise time of about 8 ns.

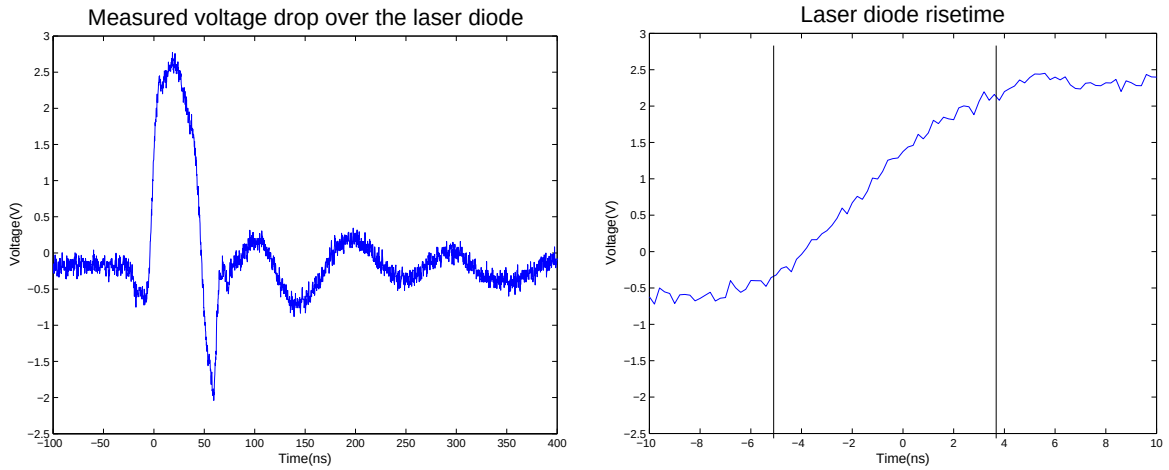

(a) Full image

(b) Highlight of the rise time

Figure 21: *Voltage drop measured over the laser diode at the moment of the pulse. The rise time can be determined from figure 21(b).*

The next method used was to look at the plot from the light power meter and check the rise time there. As seen in figure 22 the rise time is about 25 ns. Since it is known that this is a slow photo-diode (as discussed is section 3.3) this is probably not an accurate measurement of the rise time.

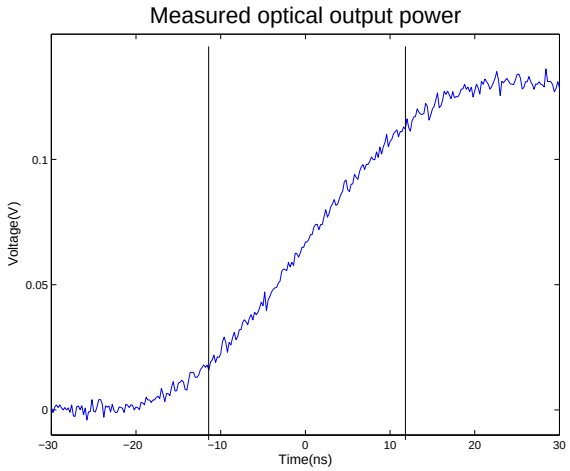

Figure 22: *A close up of the signal found in figure 19(c). The rise time is marked and estimated to about 25 ns*

The final method was to use the photo-diode on the detector board, as this would probably be a faster photo-diode than the one on the light power meter. The result shown in figure 23 shows that the rise time is about 18 ns.

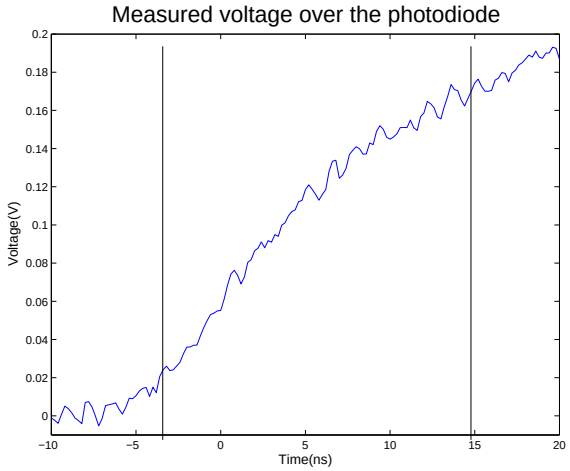

Figure 23: *The signal from the photo-diode on the detector board. The rise time marked in the figure and is estimated to be about 18 ns.*

Finally, the rise time could be determined as the fastest rise time from these three tests, which was the rise time of the voltage drop over the laser diode shown in 21(b), which was 8 ns. As mentioned before, the rise time may be shorter than this since the measurement equipment may add some rise time and since a well calibrated and fast photo-detector was not available.

Pulse length was the last parameter determined. It was verified by studying the responses in figures 19(c) and 23. The pulse length is set in software can be observed as the time from the start of the pulse (when it starts to rise) until when it starts to fall. This is of course not the real pulse length, since it would be more accurate to use the time the pulse is above a certain threshold. This means that when a pulse of a certain time is programmed, the light pulse which comes out of

the laser diode is both lagging a little bit and also shorter than programmed. However, the exact length of the pulse is really not that important to the result. Furthermore, even if the pulse is not of the correct length and is lagging, this can be compensated for, since the deviations from the programmed value are very consistent.

Furthermore, an interesting phenomenon can be seen from figure 19, especially when the power amplitude is low. The seems to oscillate at a frequency comparable to the pulse length. This is due to relaxation oscillations which at low output powers (the pumping rate is low) are of higher frequencies, which means they will show up in the window of the pulse. The reason why they don't show up when the output power is high is that the frequency of the relaxation oscillations are lower and the period of the relaxation oscillations is shorter than the pulse length.

Transmitter conclusion The transmitter works well. The laser pulse length and power can be set easily by software. The output power has a severe reduction from the maximum output power of the laser diode probably mostly due to the non-ideal collimation lens. The output power is however still almost up to the maximum allowed output power (as discussed in section 2.1.3), but the laser diode is unnecessarily strained by this. The rise time was measured to about 8 ns, which is slower than what was hoped (the laser diode has a minimum rise time of about 1 ns according to the data sheet[12]). The reason why the rise time is much larger may have several sources, such as the rise times of the MOSFETs, the control signal from the microcontroller or the rise times of the measurement equipment. The divergence of the laser beam is barely good enough to be useful in this application since the total divergence angle is equal to the wanted angular resolution for a scanning LIDAR. The hardware (especially the collimation lens) was hard to position correctly.

4.4.2 Receiver

The amplifier was hard to develop, mostly because it requires everything to be perfectly aligned. For a complete test of the receiver with a reflected signal, it first requires the laser to be working with a good collimation lens alignment. It also requires that the laser "cannon" is aimed correctly. Then, the receiver lens has to be adjusted to the correct distance from the receiver. The photo-diode of the receiver must be placed within less than millimetre a of its intended position. The fact that there is an optical light filter on the photo-diode, it is impossible to see exactly where the diode itself is located within its package. Any slight misalignment of any of these parts caused the signal to miss the detector completely.

Most experiments were therefore performed by aiming the laser directly at the photo-diode and using a low output power and optical filters to imitate the the signal power of a reflected signal. An oscilloscope was used to view the signal at different stages oft he amplifier. Unfortunately, the oscilloscope may have been a little too slow these measurements (as discussed in section 3.1).

OP-amp solution: The initial design of the amplifier using an OP-amp produced, after several iterations, some results which showed that the design was suboptimal. This was probably due to the amplifier being too slow and not able to amplify these small signals fast enough. Most of these experiments were undocumented and only served to refine the PCB and filter design. The most significant experiment performed using was a using this design was a reflection experiment that proved it was possible to use OP-amp to measure a reflection. This can be shown by the plots in figure 24. Note that these are are stylised plots since the original photos are extremely poor quality (these can however be found in figure 33(b) in the appendix). While this experiment showed that

is was possible to amplify a reflected signal, it also showed that the rise-time of the OP-amps was too long for the system to work properly over a variety of signal strengths.

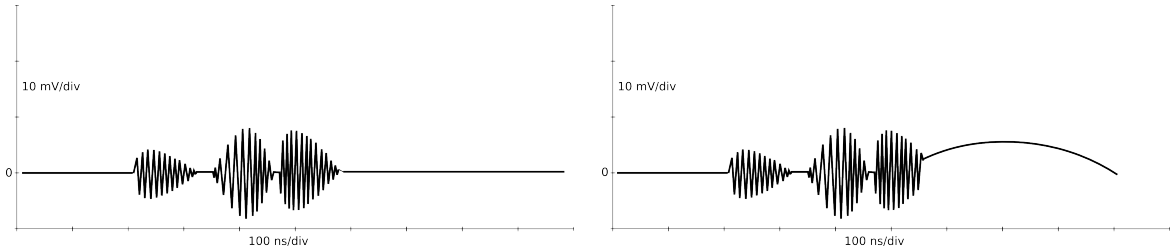

(a) With laser blocked (b) With laser active

Figure 24: *Stylised image of a reflected signal amplified by the OP-amp amplifier. It can be seen that there is lots of periodic noise, mostly due to the laser pulse travelling through the air and being picked up by the amplifier. Note that this is not a real photo or sample, since the original image was of very poor quality. The real image can be found in figure 33(b) in the appendix.*

This measurement was made using the first version of the hardware which limited the detection distance to a range of 70-80 cm due to the minimum possible distance between the transmitter and receiver blocks. Also, lots of noise can be observed in the plot. The noise source was most likely the transmitter directly interfering with the receiver. These results were the reason to develop the second version of the hardware, since it showed that the current technique could work if refined and it also showed the need for shielding for the receiver. The second version would need both the transmitter and receiver in the same module to enable measurements over a larger span as well as easier to adjust (as described in section 4.3.2).

RF-amplifier solution: As mentioned in section 4.1.2, there were several versions of the receiver boards based on RF-amplifier to test out the amplifiers and different filter configurations. Even if these did not work very well, some promising results were obtained, as shown in figure 25.

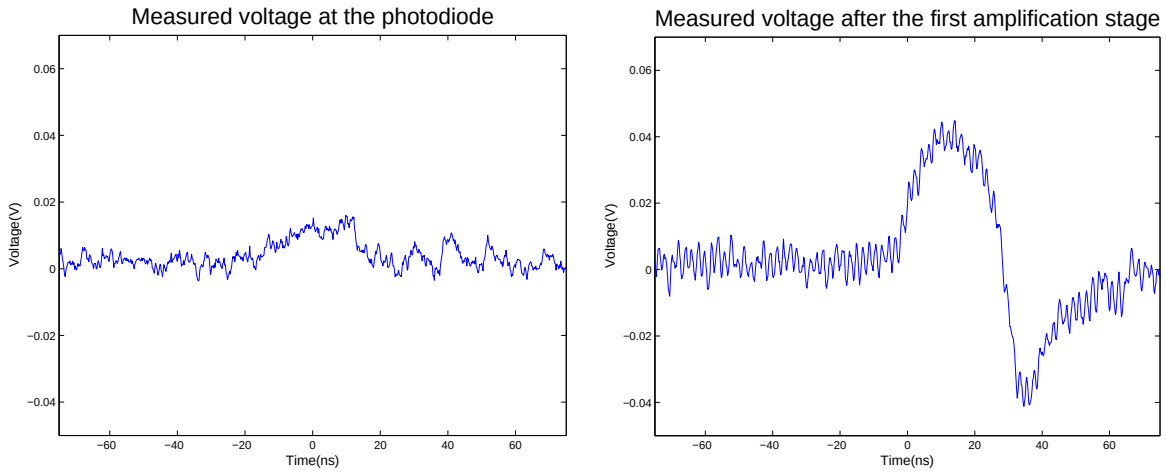

(a) Signal directly from photo-diode

(b) Signal after first amplification stage

Figure 25: *These figures shows the signal before and after the first stage of the RF-amplifier. As can be seen, the signal is barely visible in the noise (which is most likely generated in the oscilloscope) before the amplifier, but is clearly seen after the amplifier, and with severely improved rise time. This signal amplitude is about 30 times larger than the calculated minimum signal.*

This figure shows promising results. The signal is barely visible in the noise, but after the amplifier, it is clearly visible. The real worst-case signal would be about 30 times smaller than the signal observed here. It can be seen that the gain is not quite as high as advertised (the amplifier has 26 dB gain, which is equivalent to 20 times gain). One explanation may by the gain compression. It occurs when the input power to an amplifier is high and reduces the gain. It is often specified at a point when the gain decrease is 1 dB, the so called 1 dB gain compression point. This amplifier has a 1 dB gain compression of $P_{i(1dB)} = -26\ dBm$ input power, which is equal to 2.5 μW, which over an impedance of 50 Ω corresponds to an input voltage of about 11 mV. The input signal shown in figure 25(a) is about that level. The manufacturer specifies that output power at 1 dB gain compression as $P_{L(1dB)} = -3dBm = 0.5\ mW$ which corresponds to a voltage amplitude of 158 mV over a 50 Ω impedance. The output signal is not quite at 158 mV, so gain compression might not be the answer. The exact reason why the signal does not get gained up all the way is unknown.

The noise present in the figure is hard to find the source of. The noise in figure 25(a) is probably due to the oscilloscope (or probes) not being able to handle signals of this amplitude, since the same noise floor level was observed when connecting the probe directly to ground. The noise in figure 25(b) may be actual noise from the input of the amplifier, as in the high-frequency amplification of existing noise.

Receiver conclusion The receiver does not work. Generally, the testing equipment and methods were not sufficient for these kind of measurements. The detector was verified to work somewhat, but at power signals still resulting in rather long rise times. It may have worked for weaker signals, but this could not be verified using the available equipment. None of the amplifier solutions worked. Some results were obtained using the OP-amp solution, but these mostly showed that using an OP-amp based receiver was not very good due to the slow rise times. However, this was the only time a reflected signal was caught. The RF-amplifier based solution showed more promising results than the OP-amp based solution, but lots of work still remains on getting this solution to work. The noise level could not be verified due to limitations in measurement equipment. It is also unclear how

consistent the whole receiver would work given different input signal power, especially rise times and time delays. As with the transmitter, the receiver hardware was hard to position correctly, even harder than for the transmitter. The reason why it was so hard to catch a reflected signal was probably a combination of the transmitter and receiver not being aligned correctly in relation to each other.

4.4.3 Time measurement circuit

It is crucial that the time measurement circuit performs well. The circuit was tested by generating carefully timed pulses from a microcontroller and measuring the time between these pulses. Built upon this, two different methods were used to evaluate the TDC: one by varying the length of the signal path (by using different lengths of cables) and one by varying the timing between the pulses using the microcontroller. By varying the cable length, a difference in time corresponding to the increase of the signal path was observed. The times are compared against the time with no cable and used to calculate a cable length. The propagation speed of the cable was experimentally found to be about 0.66*c. This testing method did have its drawbacks. Since the signal contains very high frequencies, it is better to use shielded cable. If it is a normal cable, the signal will be capacitively transferred through the air and not travel all the way in the cable. For example, when a piece of rolled up cable was tested, it seemed as if the signal had propagated at several times the speed of light (which is obviously impossible). This capacitive transfer will however not be a problem in the real system, since the light sent through air cannot take short routes the same way the electrical signal can. Even if the signal takes short routes on the circuit board, these will be constant, and can thus be calibrated away. However, due to ease of use, normal cable of very short lengths were used. By keeping them straight all the time and not allow them to overlap the overhearing problem can be solved somewhat. Since this measurement was very noisy, not much weight will be put on it. Using heavy averaging (256 samples averaging filter), the cable length could be determined down to $\pm$ 5 mm. The other method is more reliable, since the signal only travels on the PCB, resulting an a signal much better integrity. By varying the time between the pulses using a hardware timer, very precise delays can be achieved. This method was much more extensively tested, since the goal was to test the capabilities of the TDC and not how much noise a cable generates. A total of 1 MSa was taken at 10 kHz and for different times. The results are presented in table 2 and figure 26. The samples where taken for 5 different times, with the laser on and the laser off. Testing with the laser active was deemed necessary, since it produces lots of noise, and this needed to be tested. The standard deviations are in ps.

laser state\pulse time[ns]	120	90	60	30	6
laser on	63.0360	59.7158	52.4491	32.4552	23.0415
laser off	62.0554	57.7922	71.0101	11.1349	16.2841

Table 2: *Measured standard deviations for the Time-to-Digital Circuit used in the system. Taken over a large number of samples and with the laser on and off to evaluate if the laser affects the deviation.*

As can be seen from table 2, the standard deviation is larger when the laser is on. This seems reasonable, since the laser might induce pulsed noise of high amplitude which might either propagates through the voltage supply or through the air. Furthermore the standard deviation is larger for longer times. There are multiple possible error sources for this. It could be the microcontroller clock, the TDC clock or some internal noise in the TDC. The most probable guess is that the

coarse counter in the TDC has some larger standard error, but it could be any of the other sources. The time to be measured in the real system would be below light flight-time of 10 m + delays in amplifiers and so on, so the time would be something at most 60 ns, where the standard deviation at $2\sigma \approx \pm 100\ ps$, which corresponds to ± 3 cm. This is better the wanted accuracy of ± 5 cm. Using some filters, such as a median filter, this value could be improved to get even better accuracy, as shown in figure 26.

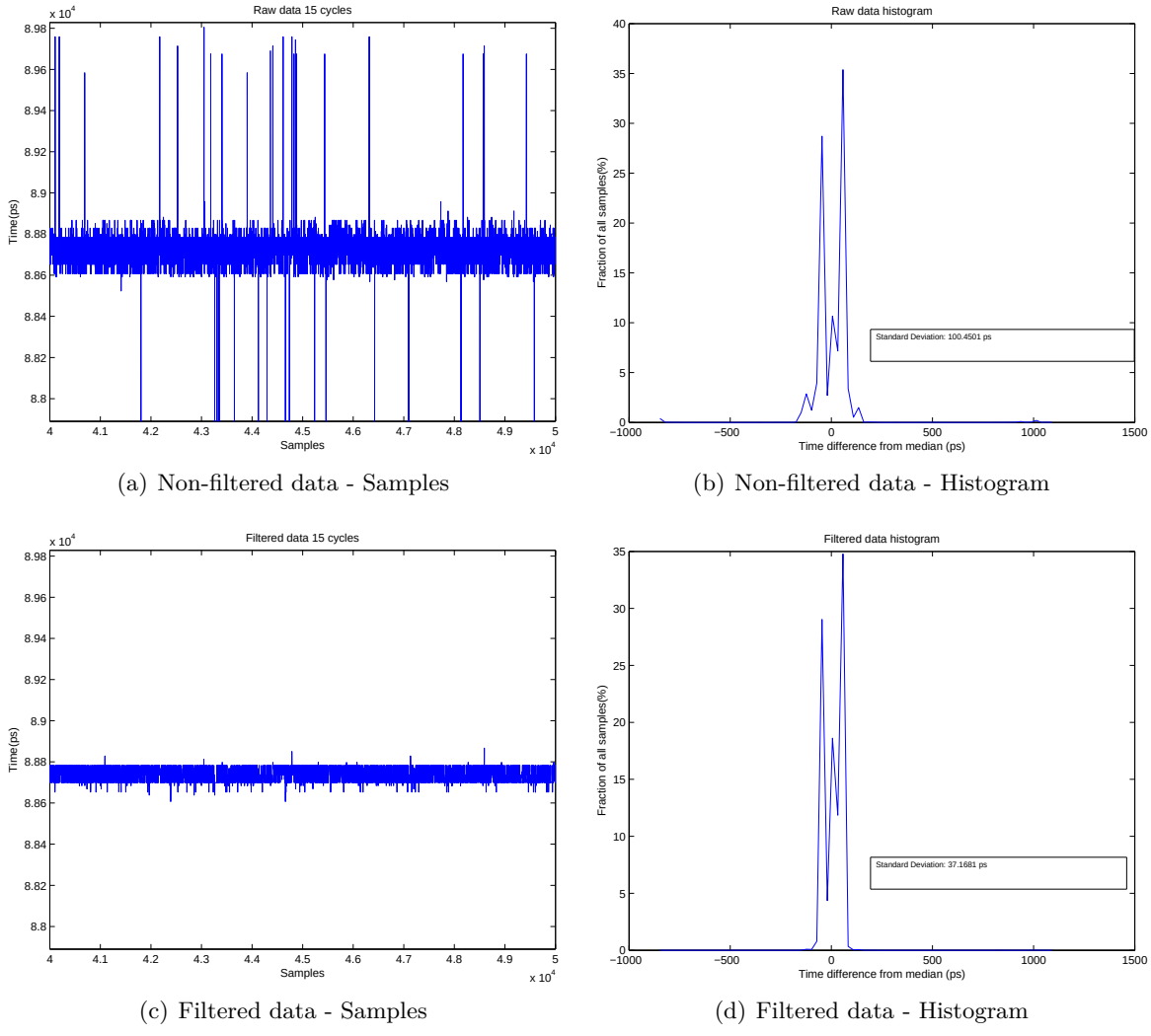

(a) Non-filtered data - Samples

(b) Non-filtered data - Histogram

(c) Filtered data - Samples

(d) Filtered data - Histogram

Figure 26: *Graphs showing the samples of the TDC, both filtered and non-filtered. These are generated by 1 million consecutive measurements, where the nominal time is about 90 ns. The filter is a simple median filter with kernel size 5. The left image shows a portion of the samples, and the right shows a histogram.*

These tests were run in the calibrated mode, where the TDC calibrates itself after each measurement. This gives a lower data rate, thus increasing the time needed to collect all samples needed for averaging. There is another mode, where the TDC does not calibrate itself between each measurement, which substantially increases data rate. However, this mode would not be more useful, since the laser should not operate at a frequency higher than 10 kHz, and one full measurement cycle in calibrated mode takes less than 10 μs (which is equivalent to 100 kHz).

The TDC also contains a noise generation feature, which provides white noise to the signal to be used when using oversampling techniques. This was however found to be very noisy (the noise generated was in the range of ± 5 ns), which means that to get a good result, an extremely long filter would be needed. The natural noise generated by the process itself was found to be enough to perform these oversampling (as mentioned before). Therefore, the built-in noise generator should not be used.

TDC conclusion The TDC works very well. It can measure times as advertised in the data sheet (down to 45 ps). Using oversampling and filters, this resolution could be improved further. The accuracy was also good. Even without filtering, the samples had a standard deviation which would satisfy the accuracy requirement (stipulated in table 1). The noise in these measurements may come from several sources, such as the microcontroller generating the pulses or the TDC generating noise. Using a median filter (even as small as 3 samples) proved to be very effective (as shown in figure 26) and severely reducing the deviation. It is clear that the TDC is not the weakest link in the system.

4.5 Cost summary

All in all the costs for all the materials very roughly approximated as shown in table 3.

Lens	€30
Laser diode	€25
Laser PCB	€45
Amplifier PCB	€15
Mechanical Materials	€10
Total cost	€125

Table 3: *Cost approximation for the LIDAR. These costs do not include manufacturing costs, which are very hard to estimate.*

The total cost of one unit is about €125. This excludes the manufacturing costs as do not take shipping, VAT and bulk prices into account. So in this aspect this goal was achieved broadly speaking. While we failed to complete a working prototype, we did complete a prototype.

5 Discussion

This project has been a bit contrary to common engineering practice in the the since that when you develop something you normally start with much better components than needed and then scale down once you know the full requirements and have gotten a prototype to work. Developing with the cheapest components needed was most likely the root of many problems during this project. This choice stems from our background with hobby development. We wanted to take the concept and work it out to try and find our way of doing it. Since the goal was something useful and cheap we went with cheap, affordable components right from the start. Given that we wanted to find our own way we also tended to look for our own solutions rather than asking others how they had done. We had prior working experience in embedded electrical design, mechanical design and microcontroller programming. High frequency analog amplification and optics are however new to us. Our own

inexperience with these subjects, in particular in high frequency amplification combined with our cheap development procedure was the main reason we feel we failed to produce a working prototype.

5.1 So what could have been done to make it work?

As mentioned earlier we chose to develop this project using cheap components. To achieve a working prototype within the time limit we should have chosen more high quality and expensive parts. For example we could have chosen a more expensive laser diode that was tested and had a tightly controlled direction and not a 5 degrees angular uncertainty in the direction it was facing. That would have reduced the headaches involved with calibrating the system by reducing the number of degrees of freedom needed on the setup.

By using a an APD, the signal might have been easier to find and less amplification needed. It would also have been more immune to noise, since the signal starts out on a high amplitude. However, extreme care would have been needed in the PCB design to manage the high voltage. This voltage also needs to be supplied, which might also present a problem. So, it is unclear if the project would actually have benefited from using an APD.

Better equipment and methods for testing the analog high-speed electronics would have been needed. The best oscilloscope available had a bandwidth of 300 MHz (and the probes probably less), which is a little slow. Furthermore, due to the lack of experience in this field, when a problem occurred, we had no idea what caused it and how it might have been fixed. More time, theory and practice would definitely have been necessary to manage to get the detector and amplifier working.

However if we had chosen the more expensive components from the start then we would most likely not have had a cheap working prototype at the end of the project. Scaling down the components in cost would most likely have been a time-consuming process even after completing a more expensive prototype.

5.2 What can be improved?

If the problems on the receiver side can be solved then all everything should be in place to make a working prototype. And once that is done and no trade-off had had to be made to reduce the sampling frequency then it could be made into a rotating LIDAR system.

6 Conclusion

LIDARs are intricate systems with many different disciplines involved, as well as being high precision and complex systems. The need for high quality and precision is the main complexity of the system, in particular for the detector, which is most likely the reason why most LIDARs are so expensive. With this project we have determined that it is most likely possible to create a functioning low-performance LIDAR at a cheap price. Although we were ultimately unable to complete such a system we have shown the possibility and where the difficulties lie so that it can be completed in the future.

7 Acknowledgements

This project has been a project with very wide focus. It would not have been possible without the help of lots of remarkable people. First, we would like to thank Thomas Vidjeskog and Göran Kvick at ÅF for giving us the chance to do this master thesis. We would also thank Lars Rymell, Leif Ek and Björn Le Normand and the other people at ÅF Technology, Optronics Division in Stockholm for their initial help with the project. Furthermore we would like to thank the people at Chalmers Robotics Society, especially Mikael Spets, Victor Påsse and Benjamin Vedder for their help with the project (especially the electronics). Also an extra special thanks to Tomas Lock who has been invaluable with his knowledge of high-speed electronics and amplifiers. We would also like to thank Sheila Galt and the others at the Photonics Department at Chalmers for helping us with the optics and letting us borrow the optics lab. A special thank to Carl-Magnus Kihlman for helping us with the first hardware prototype. A special acknowledgement goes out to the engineers at Acam for making the fantastic TDC at such a great price.

References

[1] Microsoft. *Microsoft Kinect*. URL: http://www.microsoft.com/en-us/kinectforwindows/ (Retrieved 2013-05-20).

[2] SICK. *Mätande laserscanners för inomhusbruk*. URL: http://www.sick.com/se/sv-se/home/products/product_portfolio/laser_measurement_systems/Pages/indoor_laser_measurement_technology.aspx (Retrieved 2013-05-28).

[3] Robotshop. *Laser rangefinders fron Hokuyo*. URL: http://www.robotshop.com/hokuyo-en.html (Retrieved 2013-05-28).

[4] Mouser. *THS789 - Quad channel time measurement unit, 100 ps*. URL: http://se.mouser.com/ProductDetail/Texas-Instruments/THS789PFD/?qs=%2fha2pyFaduhIPdEEqXuaOmP%252biYgrNj1G7bIxgnVmwOHjHJ6G6DUsEA%3d%3d (Retrieved 2013-05-20).

[5] Mouser. *THS788 - Quad channel time measurement unit, 13 ps*. URL: http://se.mouser.com/ProductDetail/Texas-Instruments/THS788PFD/?qs=sGAEpiMZZMuMkwKcEjFF1DDXDFJWbbmED9q%2fm0l14A0%3d (Retrieved 2013-05-20).

[6] Microchip. *AN1375 - See What You Can Do with the CTMU*. URL: http://ww1.microchip.com/downloads/en/AppNotes/CTMU%2001375a.pdf (Retrieved 2013-05-20).

[7] Wikipedia. *Triangulation*. URL: http://en.wikipedia.org/wiki/Triangulation (Retrieved 2013-05-28).

[8] TAOS. *TSL1402R - 256x1 Linear sensor with hold*. URL: http://www.ams.com/eng/content/download/250165/975693/file/TSL1402R-G.pdf (Retrieved 2013-05-20).

[9] Russell "OddBot". *Homemade Laser Rangefinder*. URL: http://letsmakerobots.com/node/2651 (Retrieved 2013-05-20).

[10] Dr. Rüdiger Paschotta. *Photodiodes*. URL: http://www.rp-photonics.com/photodiodes.html (Retrieved 2013-05-21).

[11] Wikipedia. *Photodiode*. URL: http://en.wikipedia.org/wiki/Photodiode#Materials (Retrieved 2013-05-20).

[12] Osram. *Pulsed Laser Diode in Plastic Package, 4 W Peak Power*. URL: http://catalog.osram-os.com/catalogue/catalogue.do;jsessionid=9686CABA07320E6937E4F42C8E3B4A37?act=downloadFile&favOid=020000020000a855000100b6 (Retrieved 2013-05-22).

[13] International Electrotechnical Commission. *IEC 60825 - Safety of laser products - Part 1: Equipment classification and requirements*. 2007.

[14] Laser Components. *High End / Low Cost Pulsed Laser Diodes 905D1SxxUA-Series*. URL: http://www.lasercomponents.com/fileadmin/user_upload/home/Datasheets/lcc/905d1sxxua.pdf (Retrieved 2013-05-21).

[15] Newport. *Focusing and Collimating*. URL: http://www.newport.com/Focusing-and-Collimating/141191/1033/content.aspx (Retrieved 2013-05-24).

[16] Kjell o Company. *Laserpekare med LED*. URL: http://www.kjell.com/sortiment/el/belysning/batteridrivet/ficklampor/led-ficklampor/laserpekare-med-led-p63368 (Retrieved 2013-05-24).
[17] Wikipedia. *Lambert's Cosine Law*. URL: http://en.wikipedia.org/wiki/Lambert's_cosine_law (Retrieved 2013-05-22).
[18] Edmund Optics. *Broadband Polarizing Cube Beamsplitters*. URL: http://www.edmundoptics.com/optics/beamsplitters/cube-beamsplitters/broadband-polarizing-cube-beamsplitters/2986 (Retrieved 2013-05-30).
[19] Newport. *Optics Fundamentals*. URL: http://www.newport.com/Optics-Fundamentals/604533/1033/content.aspx (Retrieved 2013-05-30).
[20] Eric W. Weisstein. *Gaussian Lens Formula*. URL: http://scienceworld.wolfram.com/physics/GaussianLensFormula.html (Retrieved 2013-05-30).
[21] Edmund Optics. *Plano-Convex Lens 25.0mm Dia. x 25.0mm FL, Uncoated*. URL: http://www.edmundoptics.com/optics/optical-lenses/plano-convex-pcx-spherical-singlet-lenses/uncoated-plano-convex-pcx-lenses/45097 (Retrieved 2013-05-30).
[22] Wikipedia. *Thin lens*. URL: http://en.wikipedia.org/wiki/Thin_lens (Retrieved 2013-05-30).
[23] Björn Gustavsson. *Opticalbench - a simple ray-tracing tool for optical systems*. 2010. URL: http://www.mathworks.com/matlabcentral/fileexchange/27412-opticalbench (Retrieved 2013-05-22).
[24] Hardik Bhavsar Van N Tran Robert Stuart. *AN3009 - Phototransistor Switching Time Analysis*. URL: http://www.cel.com/pdf/appnotes/an3009.pdf (Retrieved 2013-05-22).
[25] Mouser. *AD500-9-TO52-S1 - Pacific Silicon Sensor*. URL: http://se.mouser.com/ProductDetail/Pacific-Silicon-Sensor/AD500-9-TO52-S1/?qs=sGAEpiMZZMtWNtIk7yMEscpTFN8GTr6jUUg8bPn0aoA%3d (Retrieved 2013-05-22).
[26] Wikipedia. *Avalanche Photodiode*. URL: http://en.wikipedia.org/wiki/Avalanche_photodiode (Retrieved 2013-05-22).
[27] Texas Instruments Ron Mancini. *Op Amps For Everyone - Design reference*. 2002. URL: http://www.ti.com/lit/an/slod006b/slod006b.pdf (Retrieved 2013-06-08).
[28] Hamamatsu. "Opto-semiconductor handbook". In: *Chapter 2 - Si Photodiodes*. Hamamatsu, 2013.
[29] OSI optoelectronics. *Optical Communication Photodiodes and Receivers*. URL: http://www.osioptoelectronics.com/application-notes/AN%20Optical%20Communication%20Photodiodes%20and%20Receivers.pdf (Retrieved 2013-05-22).
[30] Wikipedia. *Rise time*. URL: http://en.wikipedia.org/wiki/Rise_time (Retrieved 2013-05-22).
[31] Wikipedia. *Bandwidth*. URL: http://en.wikipedia.org/wiki/Bandwidth_(signal_processing) (Retrieved 2013-06-03).
[32] Wikipedia. *Current-to-Voltage converter*. URL: http://en.wikipedia.org/wiki/Transimpedance_amplifier (Retrieved 2013-05-22).
[33] OSI optoelectronics. *Photodiode Characteristics and Applications*. URL: http://www.osioptoelectronics.com/application-notes/AN-Photodiode-Parameters-Characteristics.pdf (Retrieved 2013-05-22).
[34] Osram Opto Semiconductor. *SFH 203 P, SFH 203 PFA - Silicon PIN Photodiode*. 2011. URL: http://catalog.osram-os.com/catalogue/catalogue.do;jsessionid=2865064652012050440B43B83DC8B070?act=downloadFile&favOid=020000030000b636000100b6 (Retrieved 2013-05-30).
[35] Wikipedia. *Comparator*. URL: http://en.wikipedia.org/wiki/Comparator (Retrieved 2013-05-22).
[36] Texas Instruments. *LMV7219 - High speed comparator*. URL: http://www.ti.com/lit/ds/symlink/lmv7219.pdf (Retrieved 2013-05-22).
[37] Texas Instruments. *OPA2674 - Dual Wideband, High Output Current, Operational Amplifier*. URL: http://www.ti.com/lit/ds/sbos270c/sbos270c.pdf (Retrieved 2013-06-08).
[38] Mark Chen. *Phys 352 - Measurement, Instrumentation and Experiment Design - Lectures 4-5*. 2011. URL: http://www.physics.queensu.ca/~phys352/ (Retrieved 2013-06-03).
[39] Wikipedia. *JohnsonNyquist noise*. URL: http://en.wikipedia.org/wiki/Johnson%E2%80%93Nyquist_noise (Retrieved 2013-06-03).
[40] Wikipedia. *Shot noise*. URL: http://en.wikipedia.org/wiki/Shot_noise (Retrieved 2013-06-03).
[41] Wikipedia. *Amplifier - Transistor amplifier*. URL: http://en.wikipedia.org/wiki/Amplifier#Transistor_amplifiers (Retrieved 2013-05-22).

[42] NXP. *BGA2851 - MMIC Wideband amplifier*. URL: http://www.nxp.com/documents/data_sheet/BGA2851.pdf (Retrieved 2013-05-22).
[43] NXP. *BGA2818 - MMIC Wideband amplifier*. URL: http://www.nxp.com/documents/data_sheet/BGA2818.pdf (Retrieved 2013-06-08).
[44] Wikipedia. *Friis formulas for noise*. URL: http://en.wikipedia.org/wiki/Friis_formulas_for_noise (Retrieved 2013-06-08).
[45] Texas Instruments. *MSP430 - Ultra-low-power microcontrollers*. URL: http://www.ti.com/lit/sg/slab034v/slab034v.pdf.
[46] Acam. *Acam Time-to-Digital converters*. URL: http://www.acam.de/products/time-to-digital-converters/ (Retrieved 2015-06-01).
[47] ACAM. *TDC-GP21 Time-to-digital converter*. V1.4. URL: http://www.etracker.de/lnkcnt.php?et=UKbtw3&url=http://www.acam.de/fileadmin/Download/pdf/TDC/English/DB_GP21_en.pdf&lnkname=DB_GP21_en. 2012.
[48] STMicroelectronics. *STM32F407xx*. Rev 3. URL: http://www.st.com/web/en/resource/technical/document/datasheet/DM00037051.pdf. (Retrieved 2013-05-22).
[49] STMicroelectronics. *STM32F4Discovery*. URL: http://www.st.com/stm32f4-discovery (Retrieved 2013-05-22).
[50] Wikipedia. *Serial Peripheral Interface Bus*. URL: http://en.wikipedia.org/wiki/Serial_Peripheral_Interface_Bus (Retrieved 2013-05-22).
[51] OSI Optoelectronics. *Photoconductive Series*. 2013. URL: http://www.osioptoelectronics.com/Libraries/Product-Data-Sheets/Photoconductive-Photodiodes.sflb.ashx (Retrieved 2013-05-22).
[52] Wikipedia. *Polyoxymethylene*. URL: http://en.wikipedia.org/wiki/Polyoxymethylene (Retrieved 2013-05-22).

8 Appendix

8.1 Schematics

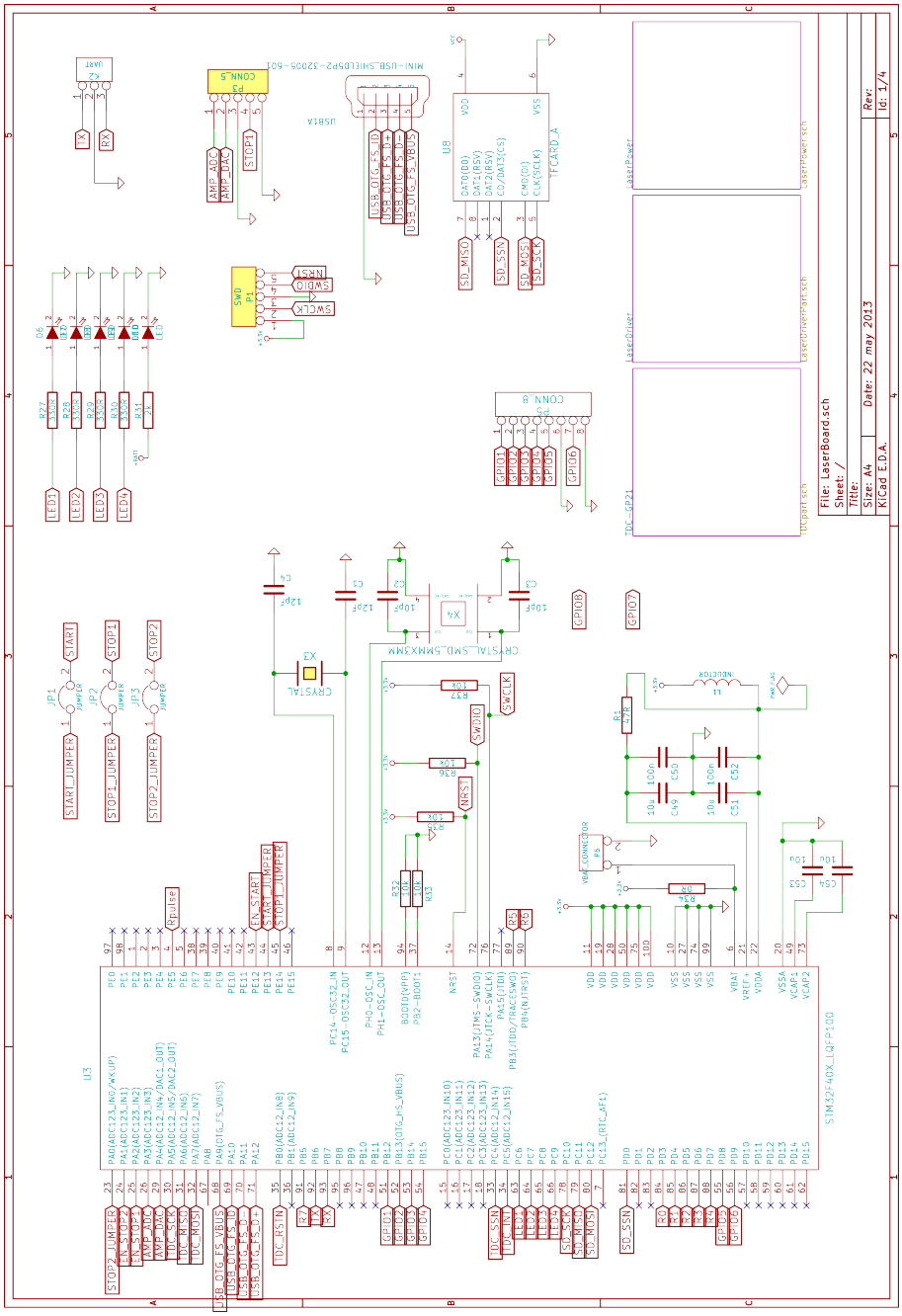

Figure 27: *The schematics of the microcontroller part of the main PCB.*

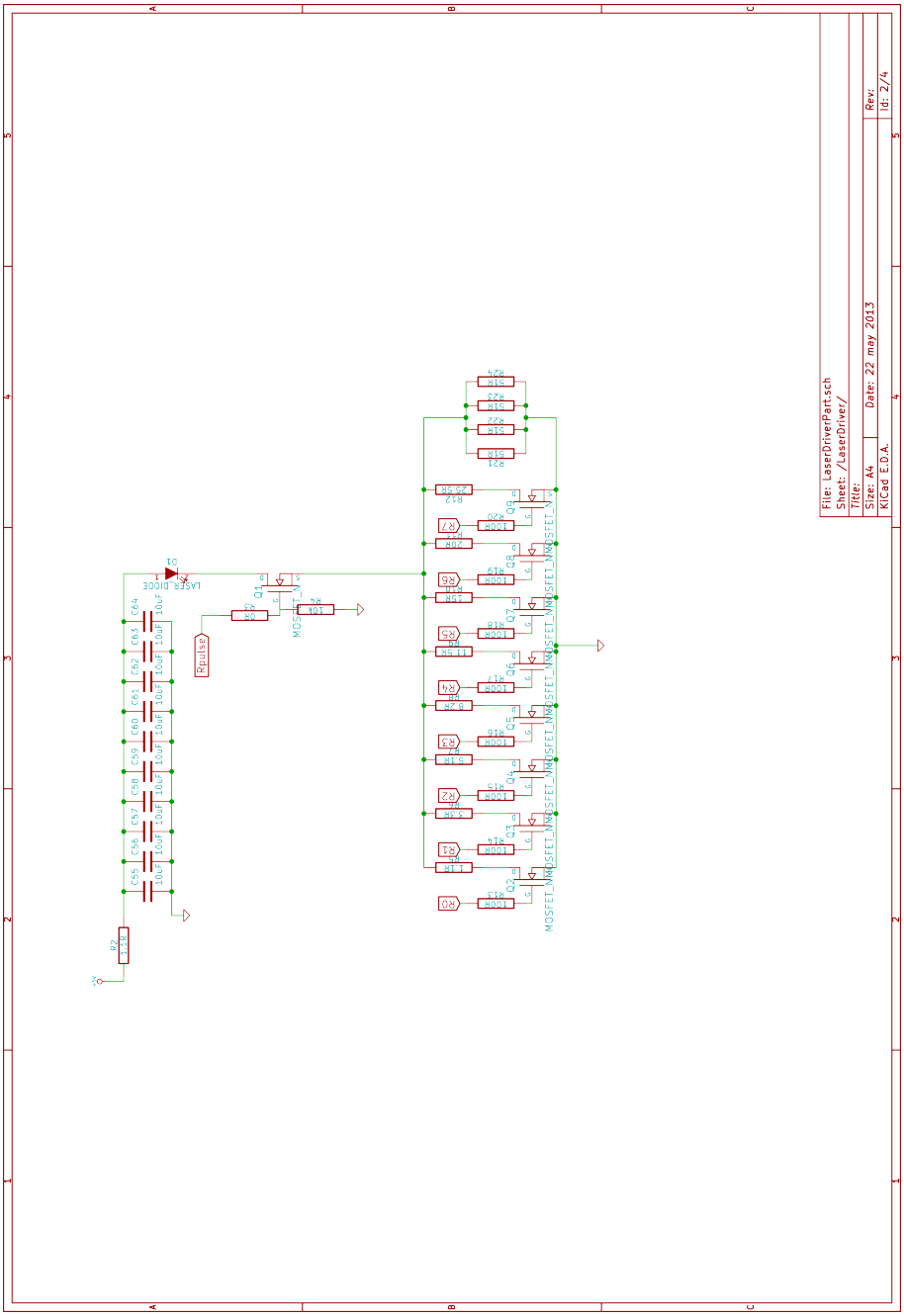

Figure 28: *The laser driver part of the main PCB.*

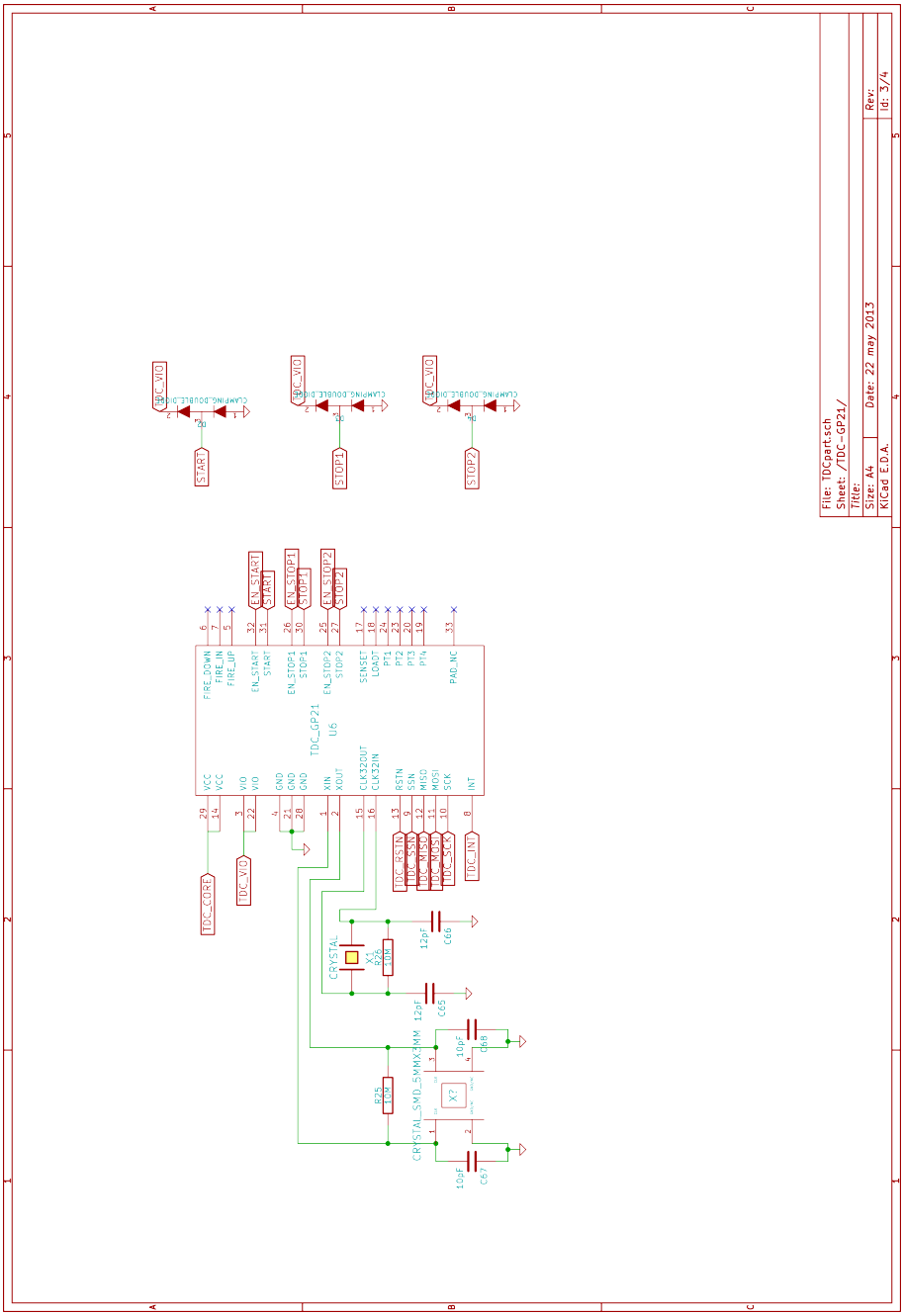

Figure 29: *The TDC-part of the main PCB.*

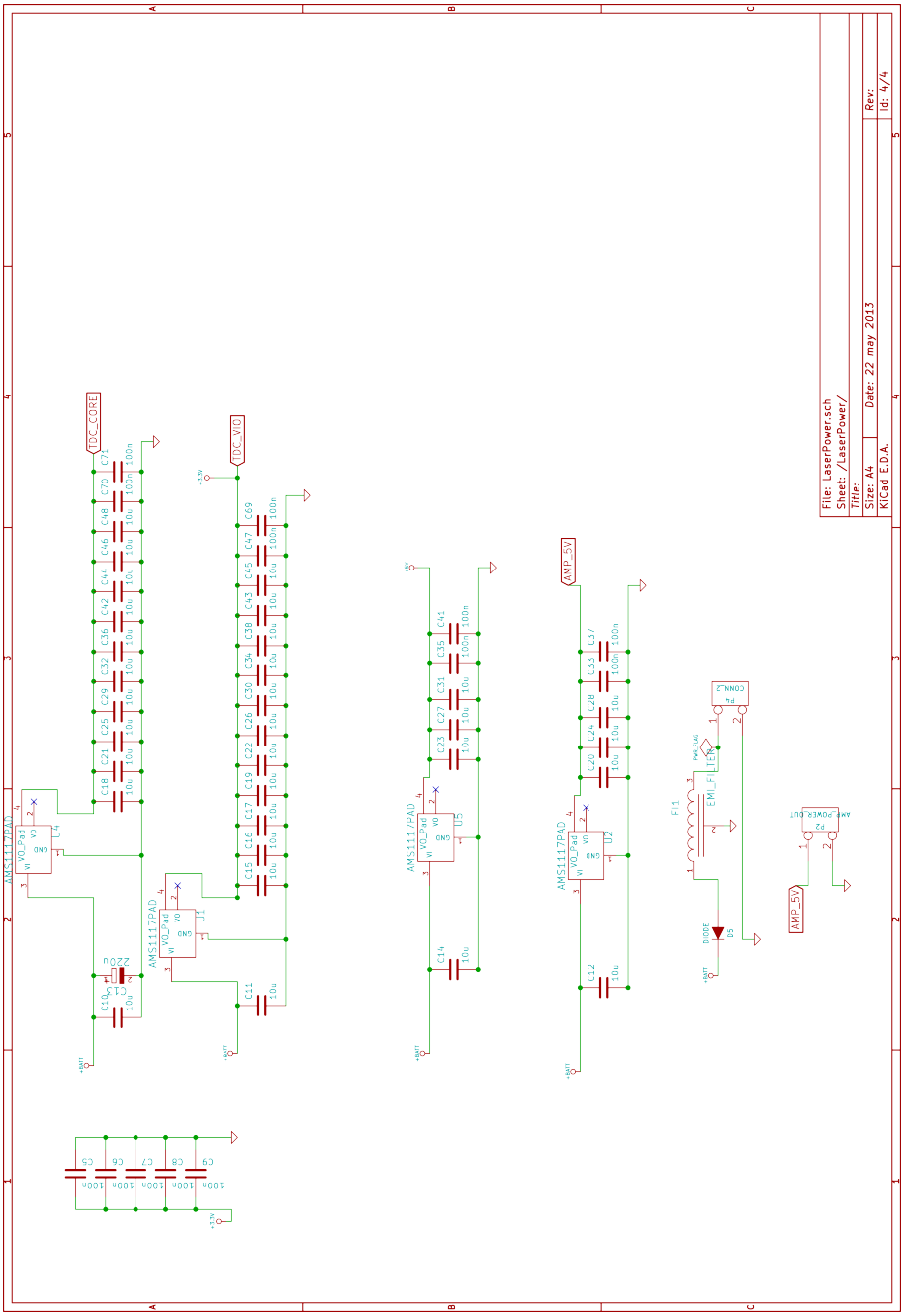

Figure 30: *The voltage regulation part of the main PCB. Many capacitors are used to ensure a voltage as smooth as possible.*

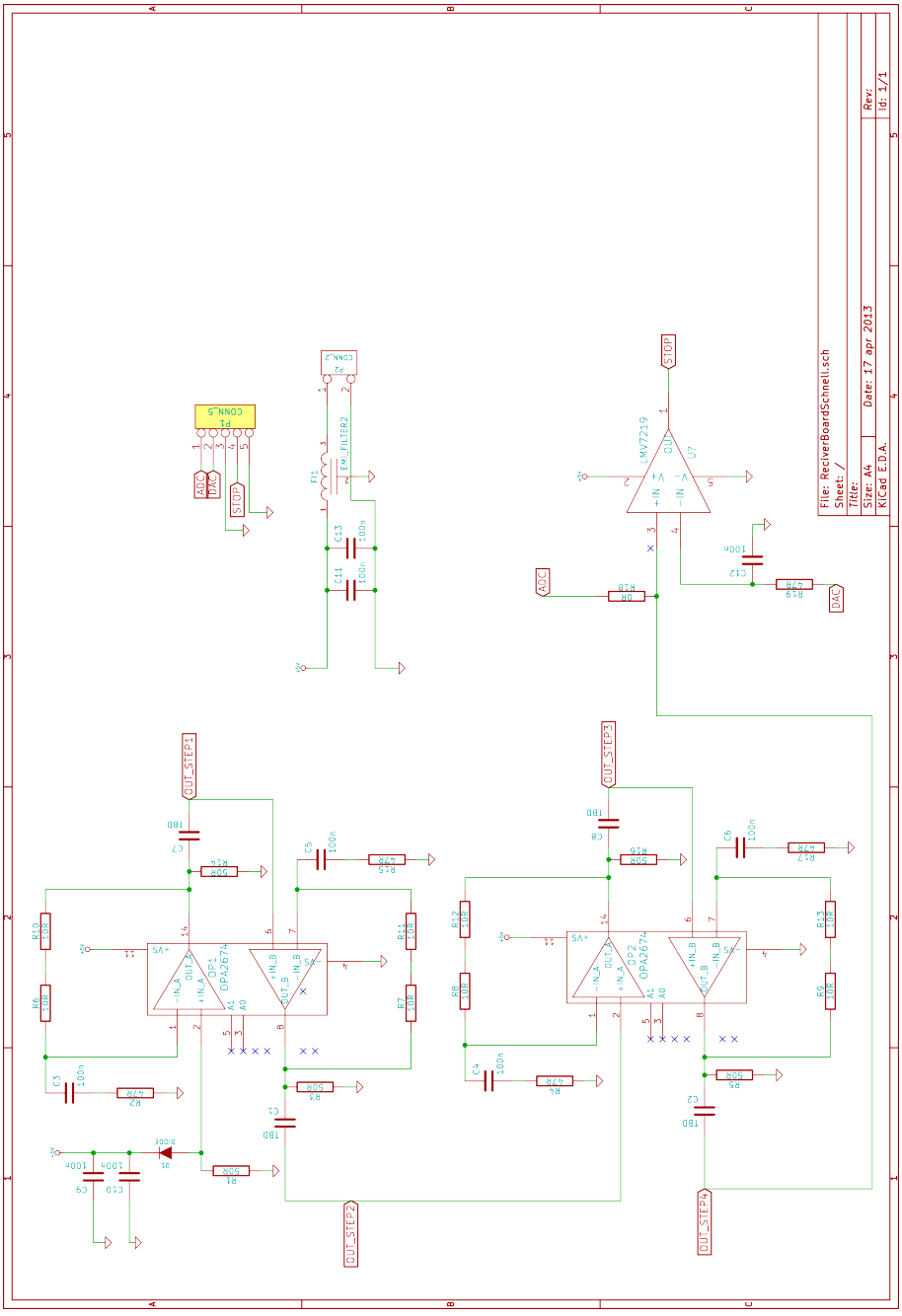

Figure 31: *The final schematics of the OP-amp receiver board.*

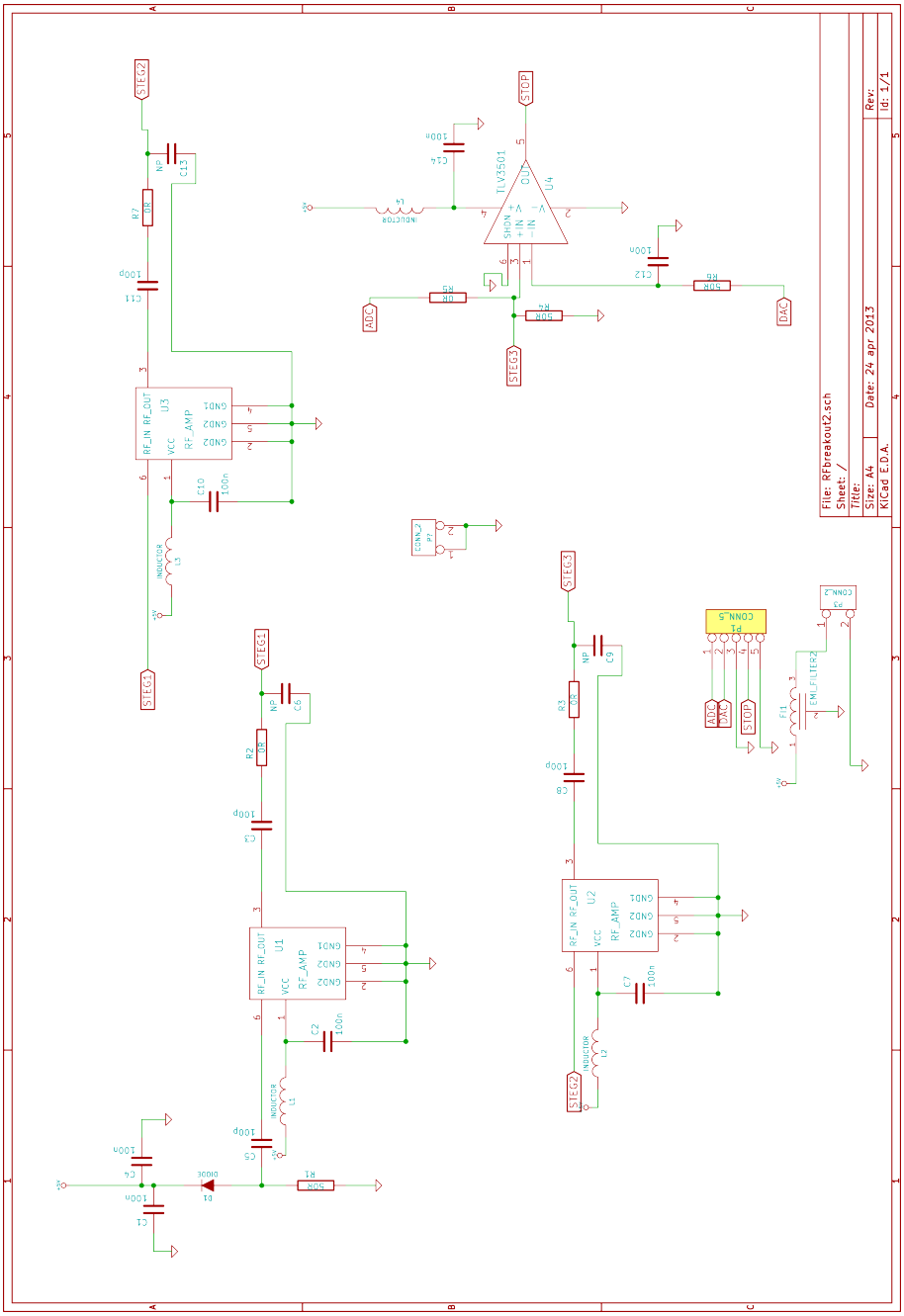

Figure 32: *The final schematics of the RF amplifier receiver board.*

8.2 Software

Most of the software is very extensive and is not supplied here (especially the C-code for the microcontroller). Furthermore, most of the software for MATLAB only generates plots. If you are interested in the code, please contact the authors.

8.2.1 MATLAB - Programmable resistor mapping

```
clc
clear

nofResistors=8;

%Max P = 5W -> Min r ? 0.5 ohm
%Min P = 0W -> MinA = 0.3A ->

R=zeros(1,nofResistors);
%for i=1:1:nofResistors
% R(i) = 2^(i-1);
%end

%Last resistor is the threshold resistor
%R = [1.1,3.3,5.1,8.2,11.5,15.0,20.0,25.5,12.75];
%R = [2.2, 2.2, 2.2, 2.2, 2.2, 2.2, 2.2, 2.2, 2.2];
R = [25.5,20.0,15.0,11.5,8.2,5.1,3.3,1.1,12.75];

Rinv = 1./R;

%Generate a truth table
truthTable = zeros(2^nofResistors,nofResistors);
for row=1:1:(2^nofResistors)
    tempRow = row;
    for col=nofResistors:-1:1
        if tempRow>=(2^(col-1))
            truthTable(row,col) = 1;
            tempRow = tempRow-2^(col-1);
        end
    end
end

truthTable = [truthTable,ones(2^nofResistors,1)]
invresult = truthTable*Rinv.';

result=(1./invresult)

result_mapping=[(1:256)', result];
[B IX] = sort(result_mapping,1,'descend')

newresult = [B , IX]

%sort(result)
```

8.2.2 MATLAB - Laser safety

```
clear
clc

c=299792458;
tp=60*10^-9; %Pulse time
lambda = 905*10^-9;
outputPower = 0.35;%[W] 1000*10^-3; %P=5mW
D=0.007; %pupil, set to 7mm
T = 100*10^-6; %[s]
f=1/T;
exptime = 30; %[s] This is only valid for t>=10s
nofPulses = f*exptime

C4=10^(0.002*(lambda*10^9-700));

MPE_single = (5*10^-3)*C4 %exposure time is 1ns - 18us (only tp is exposure time)
Ee_single=outputPower / (pi*(D/2)^2);
Ee_single*tp
if(Ee_single*tp < MPE_single)
    'Single is safe'
else
    'SINGLE NOT SAFE'
end

MPE_avg = 10*C4 %Exposure will be longer than 10s
Pavg = outputPower*tp*f;
Ee_avg = Pavg/(pi*(D/2)^2)

%MPE_avg is in W/m2
if(Ee_avg < MPE_avg)
    'Average is safe'
else
    'AVERAGE NOT SAFE'
end

Ee_single*tp
MPE_train = MPE_single*nofPulses^(-1/4)

if((Ee_single*tp)<MPE_train)
    'Train is safe'
else
    'TRAIN NOT SAFE'
end
```

8.3 Measurement data

8.3.1 Plots

Figure 33 shows a photo of the oscilloscope using the OP-amp receiver. Unfortunately, theses pictures are not of high quality, but they are the only documentation of this event available.

(a) No light signal (b) Light signal

Figure 33: *Bad photography of a the response on a reflected light signal*

Figure 34 shows the measurement circuit when measuring voltage drop over the laser diode.

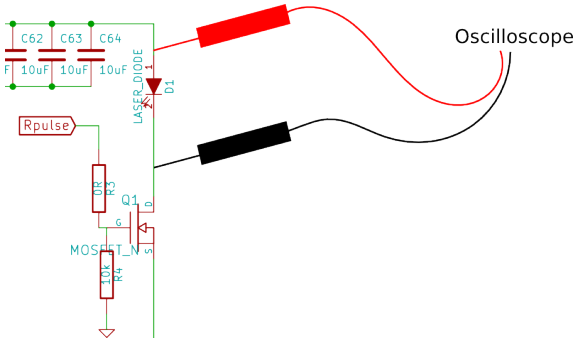

Figure 34: *Circuit when measuring voltage drop over the laser diode*

Figure 35 shows the measurement circuit when measuring the control signal to the laser pulse MOSFET

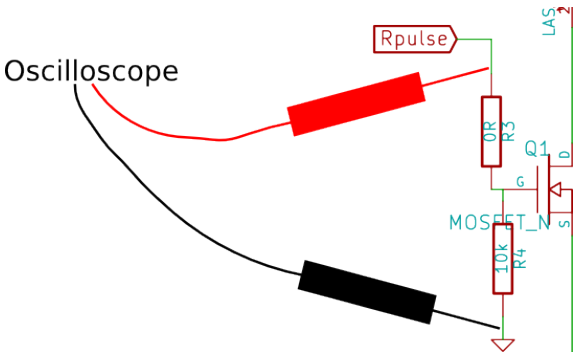

Figure 35: *Circuit when measuring the control signal to the pulse MOSFET*

8.4 List of components

Component	Part number	Vendor
Laser diode	SPL PL90_0	RS Components
Photo-diode	SFH203PFA	Mouser Electronics
Lens	Plano-Convex Lens 25 mm⌀ x 25 mm FL, Uncoated	Edmund Optics
Microcontroller	STM32F407VG	Mouser Electronics
TDC	TDC-GP21	ACAM
Opamp	OPA2674	Mouser Electronics
RFamp	BGA2851	Mouser Electronics
8 MHz Crystal	ABM3B-8.000MHZ-10-1UT	Mouser Electronics
32.768 kHz Crystal	ABS06-32.768KHz-T	Mouser Electronics
Switch MOSFET	IRFML8244TRPBF	Mouser Electronics
Resistor MOSFET	PMV22EN215	Mouser Electronics
3.3 V regulator	NX1117CE33Z,115	Mouser Electronics
5 V regulator	NX1117CE50Z,115	Mouser Electronics

Table 4: *List of components used*